Design principles of the interlocked antiphase oscillators in circadian clocks

Design principles of the interlocked antiphase oscillators in circadian clocks

概日時計におけるインターロック逆位相振動子の設計原理

PhD Thesis

Md. Mamunur Rashid

Kyushu Institute of Technology, Japan

Advisory Committee

Professor Hiroyuki Kurata, PhD advisor

Professor Tetsushi Yada

Professor Takashi Nakatsume

Professor Kazuhiro Takemoto

ABSTRACT

Design principles of the interlocked antiphase oscillators in circadian clocks

Md. Mamunur Rashid, Doctor of Philosophy

Kyushu Institute of Technology, 2020

Supervisor: Prof. Hiroyuki Kurata

In system biology, mathematical models have long tradition are used to understand complex biological control processes/ systems, for example, circadian clock oscillatory mechanism. Circadian rhythms (~24 hour) is ubiquitous in almost the living species ranging from mammals to cyanobacteria shows the robustness of key oscillatory features such as the phase, period and amplitude against external and internal variations. These autonomous oscillations are formed by the complex interactions of the interactive molecules. A transcriptional-translational feedback loop is typically characterized as a common principle for this sustained oscillations.

Recently studies, it has broadly been established that the robustness of biochemical oscillators, like the *Drosophila* circadian clocks, can be generated by interlocked transcriptional-translational feedback loops, where two negative feedback loops are coupled through mutual activations. The mechanisms by which such coupling protocols have survived out of many possible protocols remain to be revealed. To address this question, we

investigated two distinct coupling protocols: activator-coupled oscillators (ACO) and repressor-coupled oscillators (RCO).

We focused on the two coupling parameters: coupling dissociation constant and coupling time delay. Interestingly, the ACO was able to produce anti-phase or morning-evening cycles, whereas the RCO produced in-phase ones. Deterministic and stochastic analyses demonstrated that the anti-phase ACO provided greater fluctuations in amplitude not only with respect to changes in coupling parameters but also to random parameter perturbations than the in-phase RCO. Moreover, the ACO deteriorated the entrainability to the day-night master clock, whereas the RCO produced high entrainability. Considering that the real, interlocked feedback loops have evolved as the ACO, instead of the RCO, we first proposed a hypothesis that the morning-evening or anti-phase cycle is more essential for *Drosophila* than achieving the robustness and entrainability.

List of Publication

1. **Md. Mamunur Rashid**, Hiroyuki Kurata. Coupling protocol of interlocked feedback oscillators in circadian clocks. *Journal of the Royal Society Interface* in press, 2020.
2. **Md. Mamunur Rashid**, Swakkhar Shatabda, Md. Mehedi Hasan, Hiroyuki Kurata. Recent development of machine learning methods in microbial phosphorylation sites. *Current genomics* in press, 2020
3. Md. Mehedi Hasan, **Md. Mamunur Rashid**, Mst. Shamima Khatun, Hiroyuki Kurata. Computational identification of microbial phosphorylation sites by the enhanced characteristics of sequence information. *Sci. Rep.* 9:8258, 2019
4. **Md. Mamunur Rashid**, Hiroyuki Kurata; Deterministic and Stochastic Modeling of the Drosophila Circadian Clock. *Proceedings of 2nd International Conference on Applied Statistics* 2019, ISRT, University of Dhaka, Bangladesh, [P-116-I-45], Dec 27-29, 2019
5. **Md. Mamunur Rashid**, Hiroyuki Kurata; Intracellular coupled feedback loops generate anti-phase oscillators of Drosophila circadian clocks. *Proceedings of Neural Oscillation Conference* 2019, Shirankaikan, Kyoto University, Japan, Poster ID: P-04, Nov 17-19
6. **Md. Mamunur Rashid**, ABM Hasan, Yuka Umezaki, and Hiroyuki Kurata; A Coupled Feedback Oscillatory Model Provides a Robust and Entrainable Oscillator. *Proceedings of 6th International Symposium on Applied Engineering and Sciences (SAES2018)*, Kyushu Institute of Technology, Japan, Dec 15-16, 2018

Acknowledgements

First of all, I would like to thanks most merciful almighty Allah to keep me healthy and well. I would like to express my special appreciation and thanks to my supervisor **Professor Hiroyuki Kurata**, you have been a tremendous mentor for me. I would like to thank you for giving chance to engage myself in Biomedical research in the area of system biology and encouraging my research and for allowing me to grow as a research scientist. Your advice on both research as well as on my career have been priceless. My sincere thanks goes to Dr. Mehedi Hasan, Dr. Yu Matsuoka, Dr. Kazuhiro Maeda, for their generous support in this three years' journey. I would like to thank Dr. Nurul Hoque Molla for having support till today. I also like to thank the Kurata Laboratory members. I would like to thank Kyushu Institute of Technology for giving me the opportunity to attend conferences and meet so many interesting people. I gratefully acknowledge Kurata Sensei for having finance me towards my PhD course from Department of Bioscience and Bioinformatics, Faculty of Computer Science and System Engineering, Kyutech, Japan.

Special thanks to the co-supervisors Prof. Dr. Tetsushi Yada, Prof. Dr. Kazuhiro Takemoto, and Prof. Dr. Takashi Nakatsume for their insightful comments, suggestions, and encouragement during the presentations. I am always grateful to my KIT friends who help me many ways. Above all I would like to thank Dr. A.B.M. Shamim Ul Hasan for his beautiful dialogue. Last but not the least, I would like to thank my family: my father Md. Poygum Ali, mother Mst. Begum and to my brother Md. Manik for supporting me spiritually throughout writing this thesis and my life in general.

Md. Mamunur Rashid

Kyushu Institute of Technology, Japan

Table of Contents

Preface

This thesis is the final result of three years of continuous study on modeling of interconnected feedback oscillators in the circadian clock system. Motivated by the importance of a better understanding of the underlying nonlinear dynamics and robustness of circadian system, we designed and build two distinct coupling structures; the activator coupled oscillators (ACO), belong to *Drosophila* circadian system and the repressor coupled oscillators (RCO), a hypothetical one. We first demonstrate the mechanisms by which the real ACO protocols have survived out of many possible protocols by investigating this two distinct coupling protocols.

The ACO was able to produce anti-phase or morning-evening cycles; the RCO produced in-phase ones, while the ACO deteriorated the robustness of amplitude and period and the entrainability to the day-night master clock, compared with the RCO. These results lead to a hypothesis that the anti-phase cycle is more essential than achieving the robustness and entrainability.

Acronyms

ACO	: Activator Coupled Oscillators	29
SymACO	: Symmetric Activator Coupled Oscillators	34
AsymACO	: Asymmetric Activator Coupled Oscillators	34
RCO	: Repressor Coupled Oscillators	29
SymRCO	: Symmetric Repressor Coupled Oscillators	34
AsymRCO	: Asymmetric Repressor Coupled Oscillators	34

List of Figures

List of Tables

CHAPTER 1

BACKGROUND

This chapter presents the groundwork for this study. It begins with the basic terminologies of system biology/ biochemistry related to this thesis. Then, some generality has been established about feedback loops on the basis of which dynamic mathematical models of interlocked feedback loops are formed. We discuss different biological oscillators applied for circadian analysis. Finally, we briefly discuss the importance/ scope of this research.

1.1 The circadian clock and physiology

The circadian (comes from Latin *circa*, meaning "about", *dian*, meaning "day") clock instinctively integrates with all forms of life, as evidence by its role in driving physiological rhythms; such as the sleep-wake cycle, body temperature, blood pressure, periodic heartbeat and hormone secretion (Figure 1.1). This endogenous clock has a free running period approximately 24 hours that keep synchronized/ entrained the system with social cues (light) to maintain biological stability. Important properties of these clocks are autonomous means can persist even in the absence of extrinsic signals (light-dark) cycles. This indicates that the timekeeping mechanism of the circadian system is controlled by an internal clock, not by the external cycles. Recently, a growing number of studies have shown that metabolic diseases, abnormal sleep-wake cycles (e.g., Familial Advanced Sleep Phase Syndrome), and

mood disorders are highly associated with circadian clock disturbances (Xu, Toh et al. 2007, Chaix, Zarrinpar et al. 2014, Chung, Lee et al. 2014), emphasizing the clinical importance of understanding the molecular mechanisms of the circadian system (Zhang, Lahens et al. 2014).

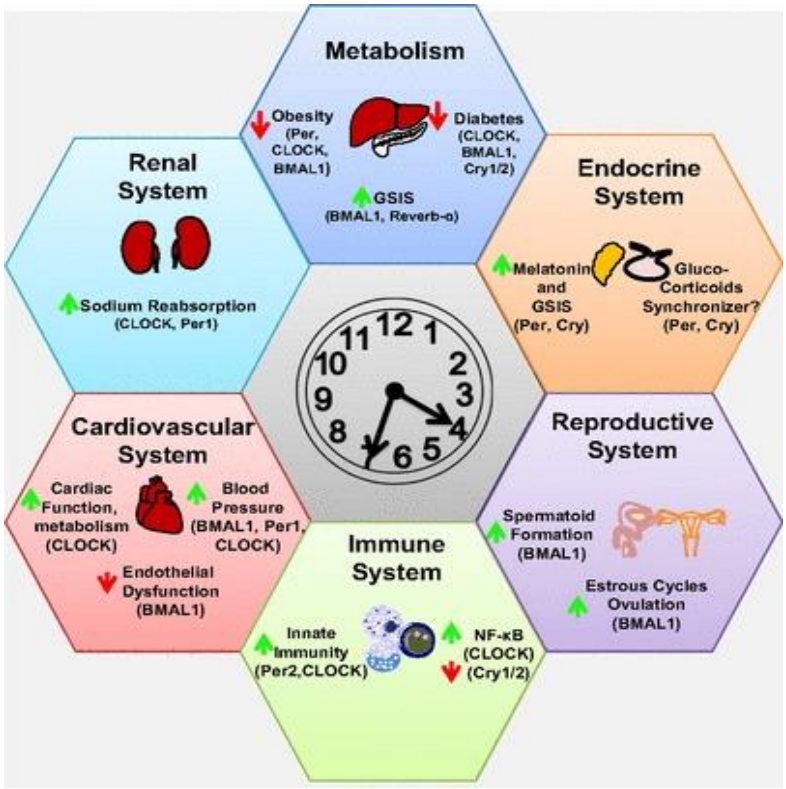

Figure 1.1. A cartoon represents the physiological functions of various organs that are integrated by the circadian clock in mammals. Circadian proteins listed in parentheses dictate which proteins have been implicated in regulating the process in question. If a protein is not listed, it does not imply that it is not involved, but that it has not yet been tested. Green arrows represent activation by the circadian protein while red one represent suppression.

The time shown on the clock is for illustrative purposes only. This figure is taken from (Richards and Gumz 2013).

1.2 The molecular basis of the circadian clocks and comparisons

The molecular mechanism responsible for generating circadian rhythms from cyanobacteria to mammals have been extensively studied in recent decades (Asgari‐Targhi and Klerman 2019, Patke, Young et al. 2019), more details can be found in this review article (Asgari‐Targhi and Klerman 2019). Naturally, circadian clocks orchestrate many biological processes to facilitate stability in physical and behavioral activities. Drosophila circadian rhythms arise from a general regulatory principle known as a negative feedback loop that is highly conserved with the molecular network of mammals (Patke, Young et al. 2019). *Drosophila melanogaster* is found to be a very well-known model organism for the investigation of the molecular nature of circadian clocks in chronobiology studies.

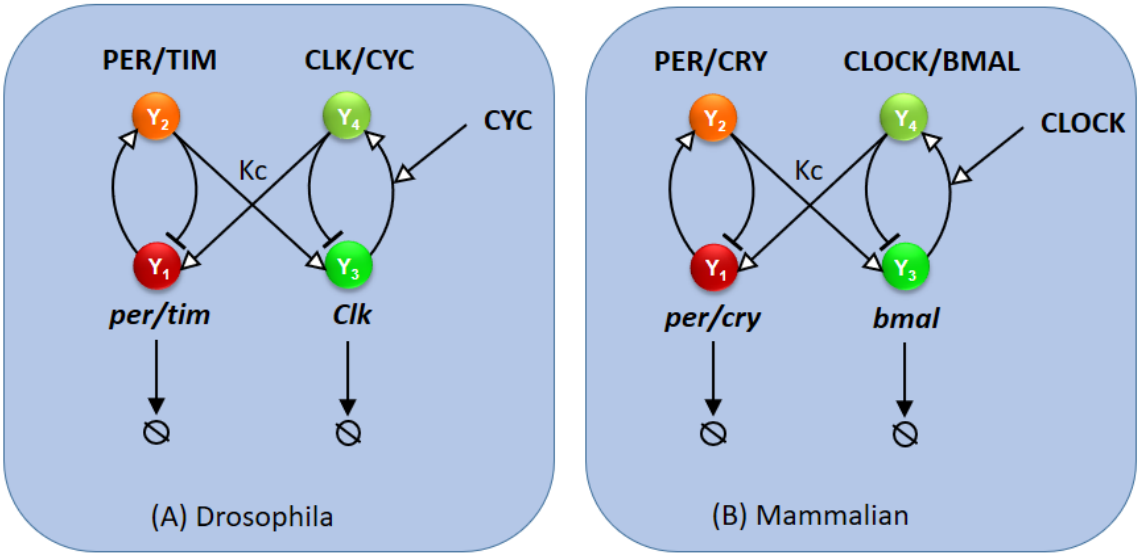

Figure 1.2. Comparison between the Drosophila and mammals circadian clock circuits. Oversimplified wiring diagram showing the interlocked transcriptional-translational feedback loop of the circadian clock network in Drosophila (A) and mammals (B).

In Drosophila, it assumed that CYCLE (CYC) proteins are abundant in the cytoplasm, of which CLOCK (CLK) protein binds to CYC and forms a protein complex, CLK: CYC is a transcription factor. CLK: CYC, the heterodimer is formed to activate the transcription-translational regulation of the target gene through two feedback loops. In the first "core" loop, the CLK/CYC target genes are period (per) and timeless (tim) (Allada, White et al. 1998, Darlington, Wager-Smith et al. 1998, Rutila, Suri et al. 1998), and in the second "interlocked" loop the target genes are vrille (vri) and Pas Domain Protein 1 (Pdp1) (Cyran, Buchsbaum et al. 2003, Glossop, Houl et al. 2003).

These positive and negative regulations are conserved in most cases in mammals where, CLK ortholog, CIRCADIAN LOCOMOTOR OUTPUT CYCLES KAPUT (CLOCK), forms a protein complex with the CYC ortholog BRAIN and MUSCLE ARNT-LIKE PROTEIN 1 (BMAL1) to form positive factors, whereas PER orthologs, PERIOD (PER1and PER2), form a heterodimer with CRYPTOCHROME (CRY1 and CRY2) instead of TIM to form the negative factor (Lowrey and Takahashi 2011). Both the CLK/CYC heterodimer and the CLOCK/BMAL1 heterodimer both are present at the main oscillatory circuits of Drosophila and mammals, respectively (Darlington, Wager-Smith et al. 1998, Leloup and Goldbeter 1998, Rutila, Suri et al. 1998).

In the core loop the CLOCK/BMAL1 target genes are Per (Per1 & Per2) and Cry (Cry1 & Cry2), in the second loop their target genes are Rev-erbs and retinoid-related orphan receptors (Rors). The first feedback loop is similar in Drosophila and mammals, with the

PER/TIM complex repressing CLK/CYC transcription in Drosophila (Bae, Lee et al. 1998, Chang and Reppert 2003) and the PER/CRY complex repressing CLOCK/BMAL1 transcription in mammals. In the second loop, PDPl activates Clk and VRI represses Clk in *Drosophila*, which is also similar to the case in mammals, as RORα activates Bmal1 and REV- ERBα represses Bmal1 (Figure 1.3) (Cyran, Buchsbaum et al. 2003, Glossop, Houl et al. 2003, Lowrey and Takahashi 2011, Chaix, Zarrinpar et al. 2014, Battogtokh and Tyson 2018, Franco, Frenkel et al. 2018).

Compared to these conserved features in Drosophila and mammals, insights into the Drosophila circadian clock will shed light on understanding mammals and human oscillations that could lead to beneficial treatments for circadian disorders and other related diseases.

1.2.1 The *Drosophila* circadian oscillator

Genetic studies in rhythmic locomotor activity and behavioral analyzes of drosophila discover molecular clock components that create two transcriptional response loops and are essential for maintaining biological time. Here I will discuss in detail the molecular mechanism of these two feedback loops.

1.2.1.1 The core feedback loop

In the core loop, also called per/tim loop, the transcription factors CLK-CYC activate the transcription of the *per* and *tim* during mid-day (Tataroglu and Emery 2014). Then, the PER and TIM begin to accumulate during the late afternoon/early evening and form a heterodimer as well (Gekakis, Saez et al. 1995, Zeng, Qian et al. 1996). During night, the accumulated level of PER-TIM protein complex binds CLK-CYC to inhibit their transcriptional activity,

and once PER and TIM are degraded early in the morning, the next round of CLK-CYC activation begins (Figure 1.3) (Hardin 2005, Allada and Chung 2010, Hardin 2011) .

Another component of this loop is cryptochrome (cry), which encodes a photoreceptor to the clock systems. CRY protein accumulates during the dark phase and declines during the day, driven by environmental light cycles. CRY binds directly to TIM in a light-dependent manner, which commits TIM to degradation (Myers, Wager-Smith et al. 1996, Zeng, Qian et al. 1996).

1.2.1.2 Interlocked feedback loop

The interlocked transcriptional feedback loop is also regulated by the core feedback loop. Two CLK-CYC-dependent transcription factors, VRI and PDP1 mediate this second transcriptional feedback loop (Glossop, Lyons et al. 1999, Allada 2003, Cyran, Buchsbaum et al. 2003, Glossop, Houl et al. 2003).

In this loop, the heterodimers CLK-CYC activate transcription of target genes vri and Pdp1. The VRI protein accumulates in phase with vri mRNA. As VRI level increases, thereby repressing Clk transcription (Cyran, Buchsbaum et al. 2003, Glossop, Houl et al. 2003) by completing the negative feedback loop. Besides with the negative feedback of VRI, PDP1 positively promote the *Clk* transcription late at night, but is not essential for *Clk* activation (Figure 1.3) (Cyran, Buchsbaum et al. 2003, Yu, Zheng et al. 2009).

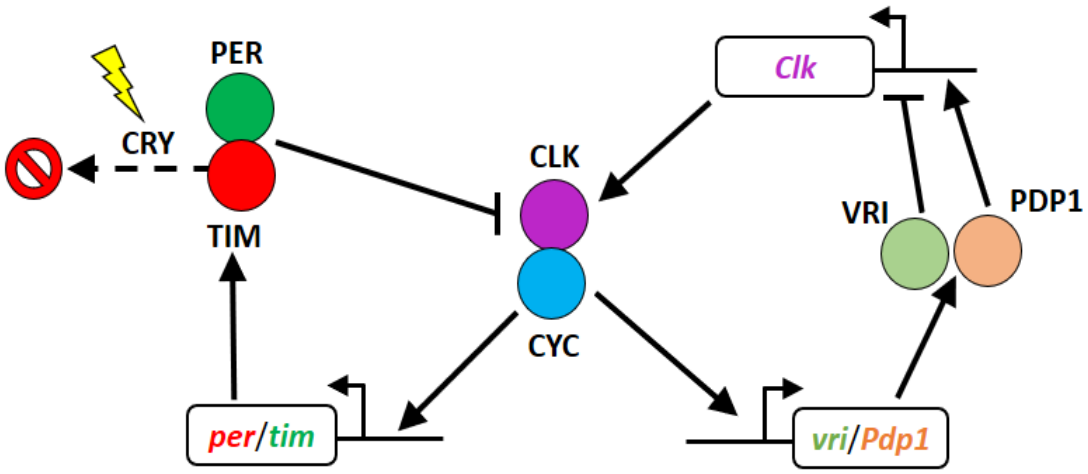

Figure 1.3. The interlocked feedback loops of the *Drosophila* clock. Two transcription feedback loops drive the *Drosophila* molecular clock. In the core loop, CLK-CYC directly activate transcription of *per* and *tim*. Inhibition of CLK-CYC activity is mediated by TIM/PER into the nucleus. In the second loop, CLK-CYC also activate *vri* and *Pdp1ε* transcription. *Clk* transcription is activated by unknown activator(s), and repressed by VRI, PDP1ε also plays a role on *Clk* transcription. Degradation of PER frees CLK-CYC to resume transcription of all the four target genes, thus restarting both loops simultaneously

1.3 Basic terminologies

To better understand circadian clock models, here, I have discussed here some basic concepts of biochemistry related to circadian oscillators. In the beginning, some concepts related to biochemical reactions that take place in the living organisms have discussed.

Typically, the biochemical reactions take place by at least two or more input substances (known as reactants) to produce a third substance (known as the product). We list the basic

chemical reactions below associated with the designed models. In the following, we indicate the reactants components by A and B and the product component by C.

1.3.1 Synthesis

The term synthesis generally relates to the creation of something. It is a biochemical reaction where at least two or more input reactants interactions form a new component. In modeling, it is often termed as production. In particular, at the cellular levels, the molecular reactions by which a protein molecule produced from the messenger RNA (mRNA), called translation. This kind of reactions occurs in the cytoplasm. Likewise, the transcription processes where mRNA molecules synthesized. This process take place in the nucleus. Generally, a solid arrow ($\rightarrow$) is used to represent the synthesis reaction aspect. For example, the transcription and translation processes can be expressed as:

$A \rightarrow C.$

1.3.2 Degradation

In the same synthesis process, degradation is another natural phenomenon in the molecular system, which is the opposite of synthesis. It is a molecular process by which an element is naturally eliminated or reduced by the influence of another element. It is also known as decomposition. A degradation process is represented using the solid arrows pointing to the symbol $\varnothing$. For example, if B is degraded, we can write this process as follow: $B \rightarrow \varnothing$

1.3.3 Regulation by activation

The activation regulatory process is importantly found in many interactive regulatory systems, for example, the circadian clock networks (Dubowy and Sehgal 2017, Jagannath,

Taylor et al. 2017). The activation process occurs when certain elements interact/bind to increase the control of a molecular process. This activation regulation can occur both on the synthesis/ degradation reactions.

For example, if an activation mechanism is involved in the synthesis process, the overall result will be an accumulation of increased amounts of the corresponding components, which is termed as a positive regulatory effect. However, if the process activates the degradation of a component, it definitely accelerates the reduction of the accumulation of the corresponding components and is termed as a negative regulatory effect. Generally, a regulatory activation effect is represented by the solid arrow lines on the component/process that is activated. For an illustration, see Figure 1.4.

1.3.4 Regulation by inhibition

Like activation regulation, inhibition mechanism plays a central role in biological negative feedback loops for producing oscillation. This process embedded a repressor effect on specific molecular reactions for a particular component.

For example, if a repression mechanism is involved in the synthesis (production) process, the overall result will be a reduced/delayed accumulation of the corresponding components, which is termed as a negative regulatory effect. Conversely, when the inhibitory process is integrated into the degradation response, it slows down the degradation process and leads to an increased accumulation of certain elements. In this case, it is called a positive regulatory effect. Generally, a regulatory inhibition effect is represented by lines with blunt ends on the component/process that is inhibited. For an illustration, see Figure 1.4.

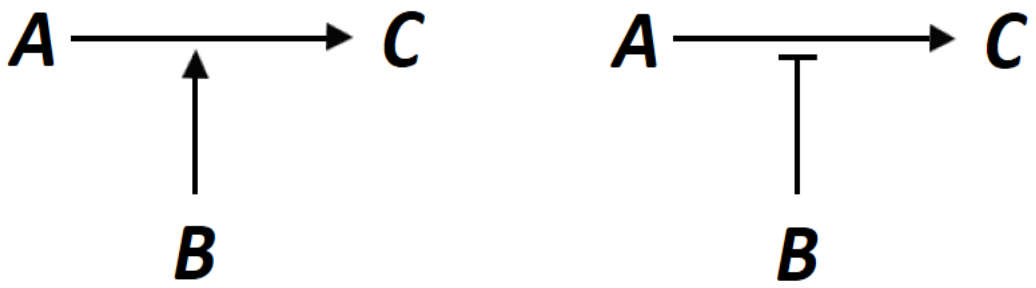

Figure 1.4. A cartoon of activation/ inhibition regulatory processes. A; B and C are the interacting molecular elements. The solid lines with arrow or blunt ends indicate the activation or inhibition process respectively. The product C is created through the synthesis reaction from reactant A. This process is activated (or enhanced) by B on the left panel, and inhibited (or suppressed) by B on the right panel.

1.3.5 Kinetic of negative and positive effect

The time course evaluation of the biochemical network models presented in this dissertation modeled using the non-linear ODE models. These regulatory systems were defined here in a similar functional framework. For modeling purposes, if no regulatory effect is involved in a molecular process, it is modeled using linear functions, otherwise, Hill-type modeling was employed to explain the control effects. In particular, at the cellular level, the positive and negative regulations for the molecular process are clearly distinguished below:

The positive regulation effect can be defined as:

$$f(P) = \frac{P^n}{K^n + P^n} \qquad (1.1)$$

The negative regulation effect can be defined as:

$$f(P) = \frac{1}{1 + \left(\frac{P}{K}\right)^n} \qquad (1.2)$$

Here, P denotes proteins, K is an activation threshold, and n is Hill coefficients of the activation (positive regulation) / inhibition (negative regulations), respectively.

1.4 Feedback loops

In biochemical networks, especially in complex molecular circuits of circadian clocks, it is important to find regulatory mechanisms to investigate the effects of specific chemical reactions that occur as a result of sequential occurrences (e.g., protein production cascade) on the system's components (olde Scheper, Klinkenberg et al. 1999, Leise and Moin 2007). This is especially true when the regulatory components influence the loss or increase of their own levels. These regulatory effects defined as Feedback loops. Typically, a feedback loop could be classified as positive or negative depending on their role in the regulation.

1.4.1 Positive feedback loop

In a biochemical system, when the outcome of a chemical process enhances/ promotes its own regulatory process, called the positive feedback system. In a positive feedback loop, an increment in one of the variables or processes can cause an increased response of another variable or process in the system. That means a positive feedback loop causes an increased accumulation of the components on which the positive regulation takes place. For more explanation, see Figure 1.5.

1.4.2 Negative feedback loop

In a biochemical system, when the outcome of a chemical process inhibits/reduces its own development process, called the negative feedback regulatory system. In a negative feedback loop, the increment in one variable or process causes a decrease in the response of another variable or process. For more details, see Figure 1.5.

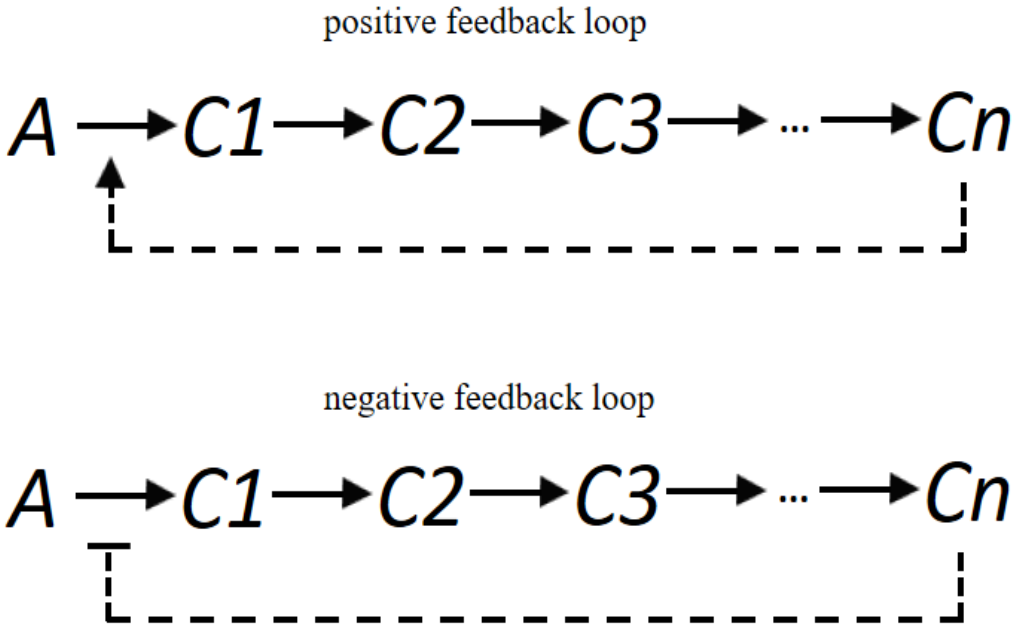

Figure 1.5. A cartoon of two feedback loops. $A, C1, ..., Cn$, are the interacting chemical elements involved in the molecular process. A produces C1, which produces C2, and so on. The final product, Cn, regulates the effect of A closing the loop. The top panel exhibits a positive feedback loop. The bottom panel exhibits a negative feedback loop.

1.5 Circadian clock features

In order to accurately characterize the functionality of a circadian oscillator, at least the following key features need to be investigated as follows:

1.5.1 Phase difference

Phase difference is defined as the synchronization state between coupled oscillators at a reference time point. The coupled oscillators with a phase difference of zero are called in-phase oscillators; those with a phase difference of half a cycle anti-phase oscillators. The other oscillators are called out-phase ones.

1.5.2 Robustness

Robustness, the ability to successfully maintain the functionality of a system to perturbation, is an indispensable feature in cellular systems (Stelling, Gilles et al. 2004, Hafner, Koeppl et al. 2009). Circadian rhythms are self-sustained oscillations, and they always show a circadian time of about 24 hours, but not equal to 24 hours, defined as a free-running period in constant conditions. The period and amplitude of circadian oscillators is said to be robust if they exhibit very less deviations after perturbation to the external fluctuations (temperature) and internal noises.

1.5.3 Zeitgeber

Circadian rhythms respond to social cues (e.g., sunlight, temperature), often referred as zeitgeber ("time giver"). The light is considered to be the strongest zeitgeber for circadian rhythms which was recruited to account for the change of the day-night cycle and seasonal variation of the environment.

1.5.4 Entrainment

Circadian rhythms show precise entrainment to 24-hour day-night external cycle (Abraham, Granada et al. 2010). Entrainment is an urgent property for adapting to a sudden variation in environment and to day-night environmental cycles (Komin, Murza et al. 2010, Pfeuty, Thommen et al. 2011). Thus, entrainment is a mechanism by which the zeitgeber can temporarily modify the endogenous (free-running) period of circadian rhythm regarding the variations of the environmental cycle. It synchronizes the internal circadian rhythm to external time cues. In mammals, the peripheral oscillators are also entrained by the SCN and exhibit synchronization of circadian oscillations during physiological events.

1.6 Scope of the present study

Circadian rhythms are integrated into all forms of life on earth. Robustness is the functional criterion of theses circadian clocks against external and internal fluctuations. Previous studies have identified "a transcriptional-translational negative feedback loop" as a key mechanism at core clock (*per-tim*) network that can produce robust circadian oscillations in constant condition, but inflexible with respect to various genetic and environmental perturbations (Ueda, Hagiwara et al. 2001, Stelling, Gilles et al. 2004, Maeda and Kurata 2012).

Several studies recently suggesting that interlocked feedback loop structures are conserved in a variety of organisms, including Drosophila and mammals, instead of a single negative feedback loop (Cheng, Yang et al. 2001, Cyran, Buchsbaum et al. 2003, Glossop, Houl et al. 2003, Stoleru, Peng et al. 2004, Akman, Rand et al. 2010, Tataroglu and Emery 2014, Battogtokh and Tyson 2018). Stelling et. al investigated the robustness of oscillatory

behaviors that are generated by complex feedback loops including dual (*per-tim*) feedback model (Stelling, Gilles et al. 2004). Maeda and Kurata further analyzed three coupled feedback loops: the dual feedback loop, semi-dual (*Clk-cyc*) feedback loop, and redundant feedback models, suggesting that the dual (*per-tim*) feedback loop provides a very robust and entrainable system (Maeda and Kurata 2012). Ueda et al. investigated the topology of two interlocked negative feedback loops including the *Drosophila* clock (*Clk)* gene expression, suggesting robust rhythmic expression (Ueda, Hagiwara et al. 2001). Smolen et. al have shown that directly interlocking positive and negative feedback loops can provide robust circadian oscillation to the parameter variations and fluctuations in *Drosophila* (Smolen, Baxter et al. 2002). Rand et. al has theoretically demonstrated that the complex interlocked loop structures increase the flexibility degree of the circadian clock network (Rand, Shulgin et al. 2006). Akman et.al. and Cheng et. al showed that greater flexibility caused by complex regulations improved the robustness of the Neurospora circadian clock's behavior (Cheng, Yang et al. 2001, Akman, Rand et al. 2010). Yan et. al showed that an increased intensity ratio of interlocked feedback loops ensures the robustness of human circadian period (Yan, Shi et al. 2014). Such coupled oscillators show entrainment to changes in temperature cycles and day-night environmental cycles (Ruoff, Christensen et al. 2005, Takeuchi, Hinohara et al. 2007, Pfeuty, Thommen et al. 2011).

All of these models produce robust oscillation properties that could explain many experimental results including mutant phenotypes. However, these models ignore important coupling protocols that are crucial for investigating the intracellular communication mechanism, as well as robustness between interconnected oscillators. Since the interlocked feedback loops have hardly been investigated in terms of coupling protocols, it raises a

critical question of how different coupling network affect oscillatory functions of phase difference, robustness of period and amplitude, and entrainment.

To elucidate how the coupling protocol evolves in the interlocked feedback loops, in this thesis, we first designed two distinct models: the activator-coupled oscillators (ACO) and repressor-coupled oscillators (RCO). The ACO has the two negative feedback loops mutually coupled by activators; the RCO implemented the two feedback loops mutually coupled by repressors (Figure 3.1AB). The ACO model is used in the *Drosophila* circadian clocks (Cyran, Buchsbaum et al. 2003, Glossop, Houl et al. 2003). The RCO model is regarded as a reference or competitive model of the ACO, which was not seen in *Drosophila* circadian clocks. For the ACO and RCO models, we performed deterministic and stochastic analyses to characterize the phase difference, robustness of period and amplitude of the ACO and RCO, which lead to a design principle by which the *Drosophila* circadian clock evolves as the ACO instead of the RCO.

1.7 Outline

This thesis is outlined in five chapters:

Chapter 1 focuses on the background of the study. The molecular basis of the circadian clock is well compared between Drosophila and mammals. This thesis gives some basic terminology of the biochemistry of the models investigated. In addition, various feedback loops and circadian clock features are briefly discussed.

Chapter 2 describes in detail the different published dynamic models. The review models have been categorizing into the two-component systems including phase oscillator, Van der

Pol oscillatory model, and the explicit delay model, and the three-component model is well known as the molecular Goodwin oscillator listed in Table 2.1. Each section presents the most remarkable features of the models regarding to the oscillation analysis.

Chapter 3 introduces two distinct interconnected coupled oscillators: the ACO and the RCO models that considered in this investigation. We employed subtle asymmetry kinetics in the systems to investigate the oscillation dynamics in terms of phase, period, and amplitude of the coupled oscillators using deterministic analyses. Deterministic analysis, reveals the two key parameters: coupling dissociation constant (K_c) and coupling time-delay (τ_c).

Chapter 4 focuses on robustness properties of the interlocked models in the context of period, amplitude and phase difference. External and stochastic noises are embedded into the systems. The impact of extrinsic noise/ parameter uncertainty on period, amplitude and phase maintenance is addressed by parameter perturbations analysis of both single and multiparameter natures. The impact of molecular noise is approached through stochastic simulations performed with the Delayed Gillespie algorithm (DSSA). Results are presented in two sections.

Chapter 5 discusses the role of network topology in terms of Entrainment/ Synchronization. With this purpose, a zeitgeber clock termed as master clock was employed to the endogenous clock network. We demonstrate that models of RCO type network possessing more robust entrainability than the network type ACO with respect to the key parameters.

CHAPTER 2

THE DYNAMIC MODELS OF CIRCADIAN RHYTHMS

In this chapter, we introduce various published dynamic models for circadian clock analysis. These published models have been categorizing into the two-component systems including phase oscillator, Van der Pol oscillatory model, and the explicit delay model, and the three-component model is well known as the molecular Goodwin oscillator listed in Table 2.1. Each section presents the most remarkable features of the models regarding to the oscillation analysis.

2.1 Introduction

Circadian clocks (approximately 24 hours) are omnipresent from single to multi-cellular levels and communication between multiple cells gives rise to physiological and behavioral features at the cellular, tissue, and system levels (Ko and Takahashi 2006, Asgari‐Targhi and Klerman 2019). Mathematical modeling has a long tradition of studying and analyzing the complex physiological systems of circadian biology (Klotter 1960, Daan and Berde 1978). Mathematical models are widely used to provide insight into circadian systems at multiple levels (i.e., organism, multi-cellular, cellular, molecular, genetic), to design new experiments, and to manipulate and control systems components in silico precisely that

cannot be easily achieved using in vivo and in vitro experimental methods for cost, time, or other reasons.

With the advancement of biotechnology, molecular biological research has matured where molecular scientists have been extremely successful in isolating the molecular interactions responsible for creating different behaviors at the cellular level under different conditions. To develop a system of dynamic models, the molecular interactions obtained from these experiments are then clearly visualized in the form interconnected nodes and directed edges. These directed edges are used to represent the positive or negative regulatory process in molecular circuits. Further, these biochemical networks are converted into a sequence of biochemical kinetic measures representing genes, proteins, metabolites, and protein dimers in order to develop precise mathematical models using mass action kinetic laws. Analysis of the dynamic properties of this model provides a better understanding of how regulatory networks and biological systems treat them. For more understanding of molecular network and mathematical models, an excellent review will find here (Beersma 2005, Gonze 2011, Gonze 2011).

Currently, the various molecular interactions that give rise to circadian oscillations are clearly identified and most mathematical models are been developed based on the molecular mechanism of expression of circadian genes. Nonlinear differential equations are very commonly used to build the mathematical models for circadian clocks, where each regulatory process follows either laws of mass action kinetics (Forger and Peskin 2003, Kim and Forger 2012) or both the mass action and enzyme kinetics (Leloup and Goldbeter 2003). These nonlinear systems are very suitable to convert into delayed models for investigating the impacts of delays in different regulatory process (Smolen, Baxter et al. 2001, Sriram and

Gopinathan 2004). These models are amenable to account the molecular noise effects on circadian clocks systems (Gonze, Halloy et al. 2002).

2.2 Two variable systems

In general, a two-variable model representing the properties of a biochemical oscillator must satisfy the following two conditions. The first is that the network must contain at least two molecular elements (e.g., cells, proteins, etc.). Indeed, models of single components with time-dependent systems are unable to generate oscillatory behaviors.

Once the systems have satisfied the first condition, the second is to the inclusion of an autocatalytic process to produce a component of the systems (Tyson 2002). Note that, a two component models incorporating either an autocatalytic process or a negative feedback loop does not guarantee to produce sustained oscillatory behaviors (Caicedo-Casso, Kang et al. 2015), thus it is essential either to include a time-delay process (Griffith 1968, Smolen, Baxter et al. 2001) or inclusion of both negative and positive feedback loops (Tyson 2002).

Considering these limitations, a number of well-known mathematical models commonly designed to simulate various properties of circadian rhythms, are reviewed in Table 2.1, each with two variables excluding the molecular Goodwin models (Eq. 2.7-2.9). Didier Gonze classified and describes these models as amplitude-phase models, abstract models, and delay models, as mentioned in Table 2.1 (Gonze 2011).

Phase oscillators, probably represent the simplest and most abstract class of models yet. The two important variables of these models are the amplitude r and the phase θ of the oscillations. Since these variables very effective in describing any rhythm of observation (no need to specify the level of protein concentration), so the equations can independently

describe the oscillating dynamics of a given system, independently of the molecular details. Phase oscillatory models helped study entrainment (Roenneberg, Dragovic et al. 2005), behaviors of coupled oscillators (Rougemont and Naef 2006, Amdaoud, Vallade et al. 2007), phase response curves (Granada and Herzel 2009), or the interpretation of experimental data (Yang, Pando et al. 2010) in a generic sense.

The van der Pol models are used to study the generic properties of circadian oscillators, originally developed in physics, where the model variables and parameters are indirectly related to molecular elements (Van der Pol 1960). These models widely applied to study resetting properties of mammalian circadian clocks (Forger, Jewett et al. 1999), investigating interactions between circadian oscillator and the cell growth (Gonze, Roussel et al. 2002), and synchronization of a population of circadian oscillators (Kunz and Achermann 2003).

Delay oscillators are useful in modeling the behavioral dynamics of circadian oscillators if the actual kinetics of intermediary processes are not relevant or unknown (olde Scheper, Klinkenberg et al. 1999, Sriram and Gopinathan 2004). The oscillatory models with explicit delay reduce the complexity of the system (in terms of models variable), yet maintain richness of dynamic behaviors (Novák and Tyson 2008).

2.3 Three variables systems

Several generic bio-molecular models of biological oscillators were presented before the molecular bases were revealed (Goodwin 1965, Pavlidis 1967, Pavlidis and Kauzmann 1969, Cummings 1975). The Goodwin model is probably the most famous one proposed in 1965 (Goodwin 1965). The Goodwin model is an abstract representation of the three component based negative feedback loop ($\mathrm{X} \rightarrow \mathrm{Y} \rightarrow Z-|\, X$) oscillators, where the final

product Z suppresses the activation of X. Although a delayed negative loop is required regarding of self-sustained oscillation, it is not sufficient, Griffith demonstrated the importance of sufficiently high nonlinearity (**Hill coefficient**) to produce sustain oscillation (Griffith 1968).

The transcription-translation negative feedback loop was first established in the early 1990s on the core of *Drosophila* and the *Neurospora* circadian clocks (Hardin, Hall et al. 1990, Aronson, Johnson et al. 1994). Later, Ruoff et al. investigated circadian properties including temperature compensation by redefining the Goodwin model, the X variable replaces by a clock gene mRNA, which then translated as protein Y and activates the production of transcriptional suppressor Z, which inhibits mRNA synthesis and completes the feedback loop (Ruoff and Rensing 1996). Goodwin published a summary of his model in 1997 (Goodwin 1997), after which, this model and its modified visions are widely used to study the interesting fundamental features of the core network of circadian oscillators including *Drosophila* and mammals (Ruoff, Vinsjevik et al. 1999, Ruoff, Loros et al. 2005, Leise and Moin 2007, Uriu and Tei 2019).

Now a days molecular based models are constantly updated to account for the dynamics of newly discovered genes and proteins rules. These models include some of the 5 to 70 variables, which stand for the concentration of genes and proteins. The kinetics of these regulatory processes such as synthesis (transcription/translation), modification (various PTM), degradation, activation, suppression, and complex binding, etc. are based on standard chemical and enzyme dynamics. Typically, the Hill equations/ Michaelis-Menten kinetics are used to describe the activation/ inhibition process, which produces sufficient non-linearity to systems (Alon 2019). Detailed molecular-based circadian clock models are

currently available for Drosophila (Leloup and Goldbeter 1998, Ueda, Hagiwara et al. 2001, Xie and Kulasiri 2007, Fathallah-Shaykh, Bona et al. 2009), mammals (Forger and Peskin 2003, Leloup and Goldbeter 2003, Battogtokh and Tyson 2018), Arabidopsis (Locke, Millar et al. 2005, Locke, Kozma‐Bognár et al. 2006), and Neurospora (Smolen, Baxter et al. 2001, Dovzhenok, Baek et al. 2015).

Other theoretical analyses, including synchronization and coupling of the suprachiasmatic nucleus (SCN) circadian oscillators, have increasingly used the Goodwin oscillators (Gonze, Bernard et al. 2005).

In addition to circadian oscillators, non-circadian oscillators (period less than 24 hours) have also been extensively studied through the recruitment of the Goodwin model, for example the Hes 1 oscillator (Lewis 2003, Soza-Ried, Öztürk et al. 2014). In particular, the choice of model approaches depends on the type of question that needs to be investigated.

Table 2.1: Types of mathematical models proposed for circadian clocks. This table is reproduce from (Gonze 2011).

Model Class	Example/ Mathematical forms
Amplitude-Phase model	$\frac{dr}{dt} = \gamma r(\alpha^2 - r^2)$ (2.1) $\frac{d\theta}{dt} = \omega$ (2.2)
Abstract model (Van der Pol)	$\frac{dX}{dt} = \frac{\pi}{12}\left(Y + \mu\left(X - \frac{4}{3}X^3\right)\right)$ (2.3) $\frac{dY}{dt} = -\frac{\pi}{12}\frac{24^2}{\tau}X$ (2.4)

Delay model	$\frac{dM}{dt} = v_1 \frac{K^m}{K^m + P_\tau^m} - v_2 M$	(2.5)
	$\frac{dP}{dt} = v_3 M - v_4 P$	(2.6)
	Where $P_\tau = P(t-\tau)$	
Molecular Model (Goodwin)	$\frac{dX}{dt} = k_1 \frac{K^n}{K^n + Z^n} - k_2 X$	(2.7)
	$\frac{dY}{dt} = k_3 X - k_4 Y$	(2.8)
	$\frac{dZ}{dt} = k_5 Y - k_6 Z$	(2.9)

2.4 Summary

In this chapter, we review several published mathematical models related to circadian clock analysis. To keep it simple and easy to understand, the models have discussed as 'two' and 'three' variable systems that are popularly used in the area of oscillatory dynamics. A further tentative classification of these models, such as phase oscillator, Van der Pol oscillatory model, delay model, and the molecular Goodwin model are listed in Table 2.1.

CHAPTER 3

MODELING THE INTERLOCKED NEGATIVE FEEDBACK LOOPS

3.1 Introduction

Circadian clocks are endogenous approximately 24-hour oscillators that regulate daily rhythms in metabolism, behavior, and physiology (Hardin 2005, Tataroglu and Emery 2014), generated by various feedback loops (Cyran, Buchsbaum et al. 2003, Glossop, Houl et al. 2003, Kurata, Tanaka et al. 2007, Novák and Tyson 2008, Gonze 2011, Bhadra, Thakkar et al. 2017). Circadian oscillators can typically be characterized by phase differences, robustness of period and amplitude, and entrainability. Phase difference has been defined as the synchronization state between coupled oscillators at a reference time point. The coupled oscillators with a phase difference of zero are called in-phase oscillators; those with a phase difference of half a cycle anti-phase oscillators. The other oscillators are called out-phase ones. Robustness, the ability to successfully maintain the functionality of a system to perturbation, is an indispensable feature in cellular systems (Stelling, Gilles et al. 2004, Hafner, Koeppl et al. 2009). If the key features of circadian clocks depend strongly on external fluctuations (temperature) and internal noises, they would not correctly predict a functional time. Robustness is the functional criterion of circadian clocks against external and internal fluctuations (Gonze, Halloy et al. 2002, Caicedo-Casso, Kang et al. 2015,

Hatakeyama and Kaneko 2015). Circadian rhythms show precise entrainment to 24-hour day-night external cycles (Abraham, Granada et al. 2010). Entrainment is an urgent property for adapting to a sudden variation in environment and to day-night environmental cycles (Komin, Murza et al. 2010, Pfeuty, Thommen et al. 2011).

Molecular mechanisms by which the circadian clocks from mammal to cyanobacteria generate the robustness have extensively been studied (Smolen, Baxter et al. 2001, Stelling, Gilles et al. 2004, Gonze, Bernard et al. 2005, Tsai, Choi et al. 2008, Akman, Rand et al. 2010, Kim, Shin et al. 2010, Pfeuty, Thommen et al. 2011). A transcriptional-translational negative feedback loop structure has been characterized as a general principle. It can provide robust oscillations in constant condition, but they are inflexible in a precise sense. Typically, simple negative feedback models alone cannot generate robustness with respect to various genetic and environmental perturbations (Ueda, Hagiwara et al. 2001, Stelling, Gilles et al. 2004, Maeda and Kurata 2012).

Many organisms including *Drosophila* (Cyran, Buchsbaum et al. 2003, Glossop, Houl et al. 2003, Stoleru, Peng et al. 2004, Tataroglu and Emery 2014), *Neurospora* (Cheng, Yang et al. 2001, Akman, Rand et al. 2010) and mammals (Kim and Forger 2012, Battogtokh and Tyson 2018) consist of multiple feedback loops. Such circadian clocks have intensively been investigated to understand some mechanisms by which different feedback loops are rationally designed for robustness. Stelling et. al investigated the robustness of oscillatory behaviors that are generated by complex feedback loops including dual (*per-tim*) feedback model (Stelling, Gilles et al. 2004). Maeda and Kurata further analyzed three coupled feedback loops: the dual feedback loop, semi-dual (*Clk-cyc*) feedback loop, and redundant feedback models, suggesting that the dual (*per-tim*) feedback loop provides a very robust

and entrainable system (Maeda and Kurata 2012). Ueda et al. investigated the topology of two interlocked negative feedback loops including the *Drosophila* clock (*Clk)* gene expression, suggesting robust rhythmic expression (Ueda, Hagiwara et al. 2001). Smolen et. al have shown that directly interlocking positive and negative feedback loops can provide robust circadian oscillation to the parameter variations and fluctuations in *Drosophila* (Smolen, Baxter et al. 2002). Interlocked feedback loops are well-known mechanisms, which exemplify the mutual interaction of the *per-tim* loop and *Clk-cyc* loop in Drosophila. Rand et. al has theoretically demonstrated that the complex interlocked loop structures increase the flexibility degree of the circadian clock network (Rand, Shulgin et al. 2006). Akman et.al. and Cheng et. al showed that greater flexibility caused by complex regulations improved the robustness of the Neurospora circadian clock's behavior (Cheng, Yang et al. 2001, Akman, Rand et al. 2010). Yan et. al showed that an increased intensity ratio of interlocked feedback loops ensures the robustness of human circadian period (Yan, Shi et al. 2014). Such coupled oscillators show entrainment to changes in temperature cycles and day-night environmental cycles (Ruoff, Christensen et al. 2005, Takeuchi, Hinohara et al. 2007, Pfeuty, Thommen et al. 2011). All of these models produce robust oscillation properties that could explain many experimental results including mutant phenotypes. However, these models ignore important coupling protocols that are crucial for investigating the intracellular communication mechanism between interconnected oscillators.

The interlocked feedback loops can be distinguished in terms of choice of coupling regulators such as activator and repressor, which determines the protocols of how different regulators are efficiently combined. A variety of coupling protocols of multiple feedback loops would create different interlocked feedback loops. There are at least two typical methods to combine two negative feedback loops: use of mutual activation or mutual

repression. Note that mutual activation and repression protocols generate a positive feedback loop, which presents bistable memory or toggle switch (Gardner, Cantor et al. 2000). Both the protocols are suggested to provide a distinct functional difference in memory persistence (Hasan and Kurata 2017). Mutual activation protocol presented more enhanced bistable memory than the mutual repression (Hasan and Kurata 2017). Since the interlocked feedback loops have hardly been investigated in terms of coupling protocols, it raises a critical question of how the mutual activation and repression protocols affect oscillatory functions of phase difference, robustness of period and amplitude, and entrainment.

To elucidate how the coupling protocol evolves in the interlocked feedback loops, in this chapter, we first designed two distinct models: the activator-coupled oscillators (ACO) and repressor-coupled oscillators (RCO). The ACO has the two negative feedback loops mutually coupled by activators; the RCO implemented the two feedback loops mutually coupled by repressors (Figure 3.1AB). The ACO model is used in the *Drosophila* circadian clocks (Cyran, Buchsbaum et al. 2003, Glossop, Houl et al. 2003). The RCO model is regarded as a reference or competitive model of the ACO, which was not seen in *Drosophila* circadian clocks. Note that the RCO is employed by the Delta-like1oscillatory gene expression system (Shimojo, Isomura et al. 2016). For the ACO and RCO models, we performed deterministic and stochastic (Chapter 4,5) analyses to characterize the phase difference, robustness of period and amplitude of the ACO and RCO, which lead to a design principle by which the *Drosophila* circadian clock evolves as the ACO instead of the RCO.

3.2 Biochemical network

The *Drosophila* circadian clock implements the interlocked feedback loops that consists of two time-delay negative feedback loops of the *per-tim* and *Clk* loops, as shown in Figure 3.1A. Both the loops are interconnected through the binding of PER:TIM and CLK:CYC, where the CLK:CYC activates the expression of the *per-tim* genes and *vri* gene (Allada 2003, Glossop, Houl et al. 2003). In the *per-tim* loops, the PER:TIM sequesters CLC:CYC away from activating *per* and *tim* expressions. Consequently, PER:TIM represses the *per* and *tim* expressions. In the *Clk* loop, CLK:CYC activates *vri* expression (Glossop, Houl et al. 2003). VRI directly represses *Clk* expression (Glossop, Houl et al. 2003). CLK:CYC can be regarded as a repressor of *Clk* expression. Those two negative feedback loops are mutually activated at gene expression level. The CLK:CYC complex activates the expression of the *per-tim* genes. On the other hand, the PER:TIM complex sequesters CLK:CYC away from activating the synthesis of VRI that represses *Clk* expression (Allada 2003, Glossop, Houl et al. 2003). Consequently, PER:TIM indirectly activates *Clk* gene expression. As shown in Figure 3.1AB, there are at least two types of coupled oscillators: one is the activator-coupled oscillator (ACO); the other the repressor-coupled oscillator (RCO). The Y_1-Y_2 oscillator stands for the *per-tim* feedback loop, and the Y_3-Y_4 oscillator represents the *Clk* feedback loop. In the *per-tim* feedback loop, Y_1 synthesis is activated by Y_4 with coupling dissociation constant K_3 and time delay τ_5. Y_3 synthesis is activated by Y_2 with K_4 and τ_6.

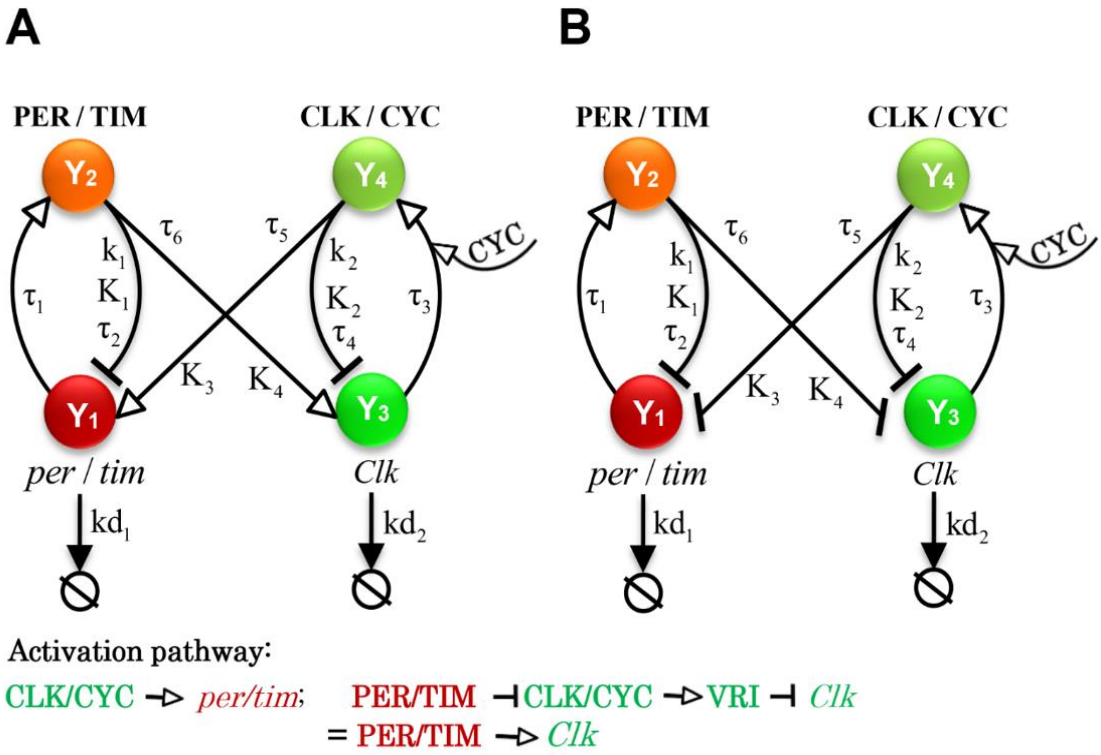

Figure 3.1 Biochemical networks of coupled oscillators and their dynamics. Two negative feedback oscillators are coupled through activators or repressors. (A) The activator-coupled oscillator (ACO) employs activators to connect two identical negative-feedback oscillators. (B) The repressor-coupled oscillator (RCO) employs repressors to connect two identical oscillators. The lines with arrows and blunt ends indicate activation and repression, respectively. (C, D) The time course of the symACO (C) and symRCO (D) were simulated. Red lines denote Y_1; green lines Y_3.

3.3 Mathematical models from biochemical networks

Since time-delay is ubiquitous in gene transcription-translation regulation and signal transduction pathways (olde Scheper, Klinkenberg et al. 1999, Lema, Golombek et al. 2000, Smolen, Baxter et al. 2001, Zavala and Marquez-Lago 2014), the negative feedback loops of *per-tim* and *Clk* definitely include a time-delay mechanism. Typically the two-variable

system cannot produce sustained oscillations (Caicedo-Casso, Kang et al. 2015), thus it is essential to include a time-delay process (Griffith 1968, Smolen, Baxter et al. 2001). Time-delay also plays a critical role in synchronization between the coupled feedback oscillators (Kim, Shin et al. 2010).

3.3.1 The ACO model

The ACO model consists of Y_1, Y_2, Y_3 and Y_4 proteins with arbitrary units (a. u.), in which Y_1 and Y_3 are considered as output components. The two negative feedback loops of Y_1-Y_2 and Y_3-Y_4 include time delays τ_1/τ_2 and τ_3/τ_4, respectively. They are mutually activated between Y_2 and Y_3 and between Y_4 and Y_1, respectively. As coupling parameters, we defined coupling dissociation constant K_3 and K_4 and coupling time-delays τ_5 and τ_6. The *Drosophila* circadian clock corresponds to the ACO model (Bae, Lee et al. 1998, Glossop, Lyons et al. 1999, Cyran, Buchsbaum et al. 2003, Glossop, Houl et al. 2003). We employed time-delayed differential equations to construct the ACO and RCO. Hill-type equations were used to provide nonlinearity to gene expression regulations. The regulators were connected with the AND logic to the repressors of the negative feedback loops. The ACO model is formulated as four variables differential equations:

$$\frac{dY_1}{dt} = b_1 + k_1 \frac{K_1^{\,n}}{K_1^{\,n} + Y_2(t-\tau_2)^n} \frac{Y_4(t-\tau_5)}{K_3 + Y_4(t-\tau_5)} - kd_1 Y_1 \tag{3.1}$$

$$\frac{dY_2}{dt} = Y_1(t-\tau_1) - Y_2 \tag{3.2}$$

$$\frac{dY_3}{dt} = b_2 + k_2 \frac{K_2^{\,n}}{K_2^{\,n} + Y_4(t-\tau_4)^n} \frac{Y_2(t-\tau_6)}{K_4 + Y_2(t-\tau_6)} - kd_2 Y_3 \tag{3.3}$$

$$\frac{dY_4}{dt} = Y_3(t-\tau_3) - Y_4 \tag{3.4}$$

where the employed kinetic parameters are described in Table 3.1.

3.3.2 The RCO model

In the RCO, the two negative Y_1-Y_2 and Y_3-Y_4 feedback loops were mutually repressed between Y_2 and Y_3 and betweenY_4 and Y_1, respectively. In the same manner as the ACO, the RCO model is formulated as four-variable differential equations:

$$\frac{dY_1}{dt} = b_1 + k_1 \frac{K_1^{\,n}}{K_1^{\,n} + Y_2(t-\tau_2)^n} \frac{K_3}{K_3 + Y_4(t-\tau_5)} - kd_1 Y_1 \tag{3.5}$$

$$\frac{dY_2}{dt} = Y_1(t-\tau_1) - Y_2 \tag{3.6}$$

$$\frac{dY_3}{dt} = b_2 + k_2 \frac{K_2^{\,n}}{K_2^{\,n} + Y_4(t-\tau_4)^n} \frac{K_4}{K_4 + Y_2(t-\tau_6)} - kd_2 Y_3 \tag{3.7}$$

$$\frac{dY_4}{dt} = Y_3(t-\tau_3) - Y_4 \tag{3.8}$$

where the employed kinetic parameters are described in Table 3.1.

3.4 Mathematical comparison

Mathematical comparison has been carried to reveal particular functional differences between competitive biochemical networks (Alves and Savageau 2000, Kurosawa, Mochizuki et al. 2002, Kurata, Tanaka et al. 2007, Hasan and Kurata 2017). It is widely recognized that oscillatory systems depend on network structure and parameter values. To compare a specific function between the competing models, we focus on the regulations critically responsible for both the models, while fixing the other functions. In this study, we selected two critical parameters: coupling dissociation constant (K_C=K_3=K_4) and coupling

time delay ($\tau_c = \tau_5 = \tau_6$), while setting the oscillation period close to 24 h, to evaluate the phase difference, the robustness of period and amplitude, and entrainability to the day-night cycle. In the ACO and RCO, the two feedback loops are the same structure except for the coupling regulations. For simplicity, we set all their corresponding kinetic parameters to the same values (Table 3.1), which is called symmetric kinetics. In addition, we defined the subtle asymmetric kinetics by 10% changing degradation rate constant kd_1 of the Y_1-Y_2 loops, because the symmetric kinetics are unlikely to exist in real, interlocked feedback loops. The ACO with symmetric kinetics and the RCO with symmetric kinetics are named the symACO and symRCO, respectively. The ACO with subtle asymmetric kinetics and the RCO with subtle asymmetric kinetics are named asymACO and asymRCO, respectively.

3.5 Simulation

3.5.1 Time delay differential equation

Since a transcriptional-translational process involves a time-delay event, we adopted time delay differential equations. Both the ACO (equations 3.1-3.4) and RCO (equations 3.5-3.8) equations are numerically integrated with delay differential equation solver 'dde23' (MATLAB R2018a, Mathworks). All computational analyses were carried out on MATLAB.

3.5.2 Measure of the circadian key parameters

The period and amplitude of the coupled oscillators are defined as:

$$Period = T_{j,top}(i) - T_{j,top}(i+1) \tag{3.9}$$

$$Amplitude = Y_{j,top}(i) - Y_{j,bottom}(i) \tag{3.10}$$

where j (=1,2,3,4) is the protein index, $T_{j,top}$ represents the top peak time of protein j, $Y_{j,top}$ and $Y_{j,bottom}$ indicate the top and bottom concentrations of protein j, and i is the index of the sequential peaks. Phase difference between Y_1 and Y_3 is expressed at a particular time point as:

$$Phase\ difference = \left| \frac{T_{1,top}(i) - T_{3,top}(i)}{T_{1,top}(i) - T_{1,top}(i+1)} \right| \qquad (3.11)$$

In deterministic analysis, the top and bottom peak times were detected using the "findpeaks" build-in MATLAB function.

Table 3.1: Parameter values for the ACO and RCO models

Kinetic parameter	**Name**	**Value**	
		ACO	**RCO**
$K_c = K_3 = K_4$	Coupling dissociation constant	0.60	0.60
$\tau_c = \tau_5 = \tau_6$	Coupling time delay	5	5
b_1=b_2	Basal synthesis rate constant	0.01	0.01
$k_1 = k_2$	Synthesis rate constant	10	10
kd_1	Degradation rate constant	0.95	1.13
kd_2	Degradation rate constant	0.95	1.13
$K_1 = K_2$	Dissociation constant	1	1
$\tau_1 = \tau_3$	Time delay	5	5
$\tau_2 = \tau_4$	Time delay	5	5
n	Hill coefficient	2	2

3.6 Results

3.6.1 Time course of the symACO and symRCO

We simulated the deterministic dynamics of both the symACO and symRCO, as shown in Figure 3.2, where the corresponding kinetic parameters between the coupled oscillators are set to the same values. Both the models produced in-phase oscillations with a period of 24 hours, while the ACO and RCO models provided low and high amplitudes of 3.26 (a.u.), and 8.51 (a.u.), respectively.

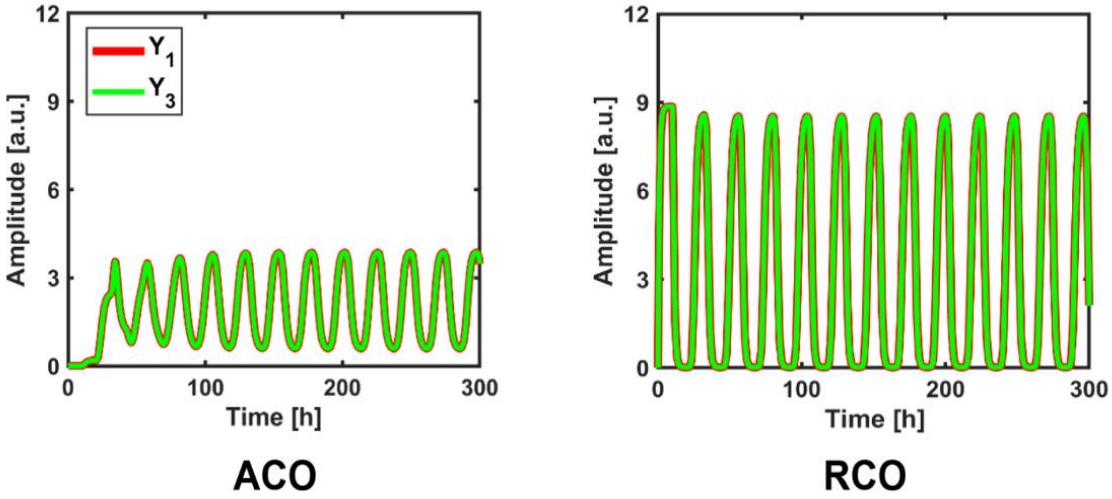

Figure 3.2 Time course of the coupled oscillators: the symACO model and the symRCO model were simulated. The employed symmetry parameters are listed in Table 3.1.

3.6.2 Coupled oscillator with subtle asymmetric kinetics

Along with period and amplitude, the phase difference is a key feature of the coupled oscillators (Pfeuty, Thommen et al. 2011, Bordyugov, Abraham et al. 2015, Hatakeyama and Kaneko 2015). We perturbed the single parameter of degradation rate constant kd_1 by 10%, while setting the other corresponding parameter values to the same ones between the ACO and RCO, to construct the asymACO and the asymRCO. Interestingly, a very small

variation of kd_1 readily changed the in-phase ACO into the anti-phase ACO (Figure 3.3A), while it did not cause any phase shift in the RCO (Figure 3.3C). As shown in Figure 3.3B, D, both the ACO and RCO oscillated with a period of 24 hour and with a high amplitude. The asymACO readily oscillates with a higher amplitude than the symACO.

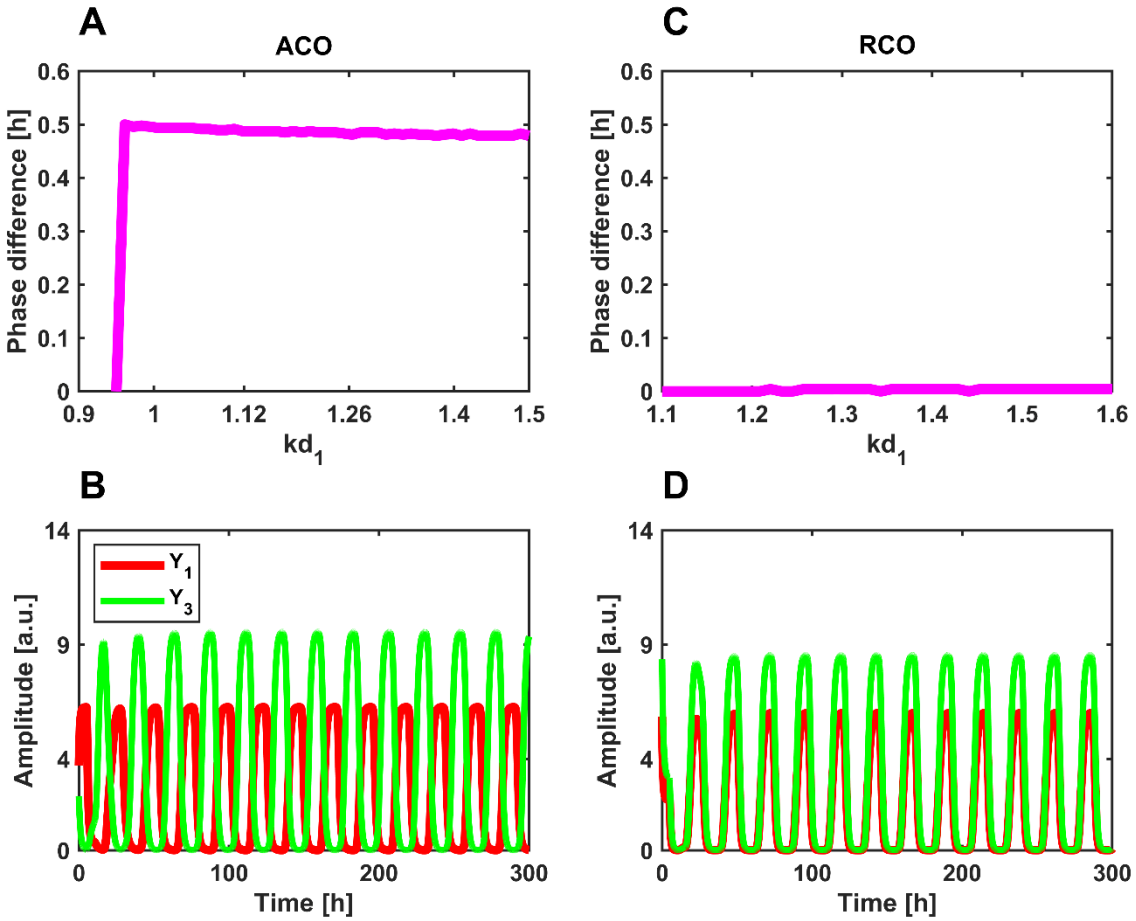

Figure 3.3. Effect of single parameter perturbation on the phase difference between the coupled oscillators. To evaluate the phase shift between the coupled oscillators, we varied the value of degradation rate constant kd_1, which gives subtle asymmetric kinetics to the ACO and RCO. The employed kinetic parameters are listed in Table 3.1. (A) The phase difference of asymACO. (B) The distinct anti-phase oscillators are produced when subtle asymmetric kinetics is given. (C) The phase difference of asymRCO. (D) The distinct in-phase oscillators remain when a subtle asymmetric kinetics is given.

3.6.3 Effect of coupling time-delay and coupling dissociation constant on phase transition

To understand how asymmetric kinetics reverses the phase of the ACO, we focused on the two key parameters, the coupling time delay (τ_c) and coupling dissociation constant (K_c), and simulated the oscillatory features of both the asymACO and asymRCO, as shown in Figure 3.4. Both of them provided two distinct phases, depending on the two coupling parameters (Figure 3.4 AD). The ACO produced the anti-phase oscillators within a specific region of τ_c =0.10-9.60 hour and K_c =0.01-1.90 (a.u.), and provided an in-phase oscillator for τ_c >9.6 or K_c >1.90. The RCO exhibited the opposing behaviors to the ACO. The RCO produced an in-phase oscillator in a region of τ_c = 0.10-12.10 and K_c = 0.01-2.40 and presented an anti-phase oscillator in a region of τ_c >12.10 h or K_c >2.40 (Figure 3.4D). The period and amplitude greatly changed around the transition regions where the phase shift occurred (Figure 3.4B, C, E, F).

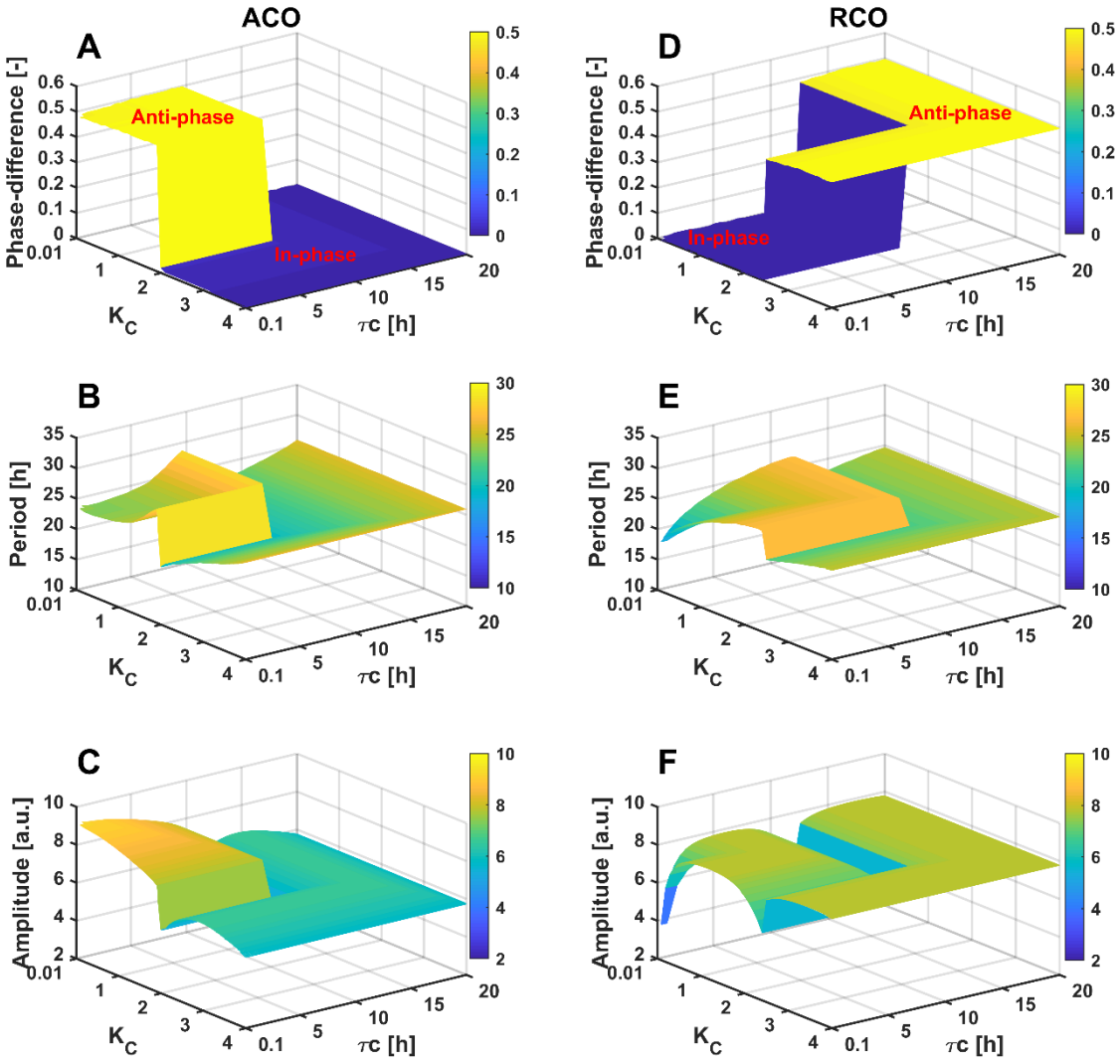

Figure 3.4. Phase difference, period and amplitude of the ACO and RCO. We varied two key coupling parameters: the coupling dissociation constant (K_C) and coupling time delay ($\tau_c = \tau_5 = \tau_6$). The employed kinetic parameters are listed in Table 3.1. The asymACO and asymRCO were used. (A, B, C). The phase difference, period and amplitude of the asymACO are simulated with respect to the two key coupling parameters. (D, E, F). The phase difference, period and amplitude of the asymRCO are simulated with respect to the two key coupling parameters.

3.7 Discussion and conclusion

In this chapter, we first simplify the interlocking feedback system of the *Drosophila* circadian clock and design two distinct coupled oscillators: the ACO and the RCO models. We investigate the effect of subtle asymmetry kinetics on the dynamics (the phase, period and amplitude) of the oscillators. Both the symACO and symRCO provided in-phase oscillations (Figure 3.2), while the asymACO was changed to anti-phase oscillators (Figs. 3.3 and 3.4), depending on coupling dissociation constant and coupling time-delay.

The ACO presented an anti-phase and in-phase oscillator at τ_c < 9.6 hour and at τ_c > 9.6 hour, respectively. In practice, it is likely that time-delay in transcription-translation processes is less than 9.6 hour and that the kinetics is asymmetry between the two feedback loops because the biological reactions of each loop are definitely different. Considering the realistic time-delay and asymmetric kinetics, it is reasonable that the ACO shows the anti-phase oscillator. In the same manner, it is reasonable that the RCO with realistic time-delay presents the in-phase oscillator. Deterministic analysis of asymACO and asymRCO, indicated that the circadian period and amplitude of the ACO was less robust than that of the RCO.

CHAPTER 4

ROBUSTNESS OF THE INTERLOCKED CIRCADIAN OSCILLATORS

4.1 Introduction

Biochemical oscillators have many interesting and distinctive features, the most obvious one is robustness, (Barkai and Leibler 1997, Stelling, Gilles et al. 2004, Barkai and Shilo 2007, Kurata, Tanaka et al. 2007). Robustness, the ability to successfully maintain the functionality of a system to perturbation, is an indispensable feature in cellular systems. Stochasticity is a predominant disturbance in biochemical reactions that impacting biological systems arising due to the discreteness of molecular entities. Typically, a large copy of a molecule hardly affects the properties of a system, but a system with a small copy of a molecule (e.g., low copy mRNA species) can produce significant stochasticity (Ozbudak, Thattai et al. 2002, Swain, Elowitz et al. 2002, Bar-Even, Paulsson et al. 2006). In living cells, the circadian clock system is ruled by a complex interconnected biochemical network that is determined by random interaction of molecular components exhibit variations in gene expression (Swain, Elowitz et al. 2002, Kaern, Elston et al. 2005, Gillespie 2007, Munsky, Neuert et al. 2012). Thus, even the fluctuations of a single component can potentially impact the performance of an entire system.

In addition to internal noise, the outcomes of biological oscillations may be influenced by changes in the cellular environment, and by the uncertainty of parameters called extrinsic/ external noise (Singh and Soltani 2013, Caicedo-Casso, Kang et al. 2015). Basically the disturbances of circadian rhythms can categories into intrinsic/ stochastic noise and extrinsic/ external noise (Hilfinger and Paulsson 2011). Many experimental and systems biologists have rigorously investigated the system's robustness using a variety of perturbations techniques (Wagner 2005, Barkai and Shilo 2007, Kurata, Tanaka et al. 2007, Maeda and Kurata 2011).

Circadian rhythms are endogenous clocks, maintain the robustness of physiology and behavioral functions of all levels of biological systems at different sources of fluctuations (e.g., temperature changes and molecular noise). Key parameters such as phase, period, and amplitude have been extensively studied to distinguish the robustness of circadian rhythms in different organisms (Smolen, Hardin et al. 2004, Stelling, Gilles et al. 2004, Locke, Millar et al. 2005, Akman, Rand et al. 2010, Caicedo-Casso, Kang et al. 2015, Hatakeyama and Kaneko 2015, Putker, Crosby et al. 2018). For example, the robustness of the *Drosophila* circadian system has been identified by investigating the circadian period to temperature compensation and temperature sensing, and nutrient compensation (Kidd, Young et al. 2015, Williams, McCue et al. 2016, Rendon, Walton et al. 2019).

This chapter aims to investigate the robustness of key oscillatory features such as phase, period, and amplitude using the interlocked ACO and RCO models described in chapter 3. This analysis is carried out by assigning two different types of disturbances. First, external fluctuations are incorporated into the systems by analyzing the multiparameter perturbation/ global sensitivity of kinetic parameters. Multi-parameter perturbation technique explains the

environmental or cell to cell variations that can affect the behavior of a system. Second, considering the real stochastic nature of circadian oscillators, molecular noise is embedded in both models using the delayed stochastic simulation algorithm (DSSA).

4.2 Robustness to the external noise

Heterogeneity is a well-known underlying phenomenon of biochemical oscillators. This heterogeneity is derived by both the external and internal sources of noise (Singh and Soltani 2013). In this section we focus on the effects of external noise, defined as variability arising from environmental fluctuations, for example, temperature changes, cell-to-cell differences, feeding disturbances, etc. As a result of these fluctuations, the rate of chemical reactions associated with the molecular network of circadian clocks may be modified. Thus, variations in the phenotype of the oscillatory system may observe due to the rapid or slow speed of chemical reactions. A well-known technique to examine the effect of external fluctuations on the behavior of biological systems is systematic variations of parameter space (Leloup and Goldbeter 1997, Leloup and Goldbeter 2003, Stelling, Gilles et al. 2004). Here, we investigate the robustness of phase, period and amplitude using the ACO and the RCO models described in chapter 3. Typically, the system's parameters can be varied in two ways: single parameter sensitivity analysis, where only a subset of parameter spaces are embedded with disturbances to probe robustness (Wolf, Becker-Weimann et al. 2005) and the other is multiparameter perturbation analysis where all the rate kinetics simultaneously varies randomly across the entire system (Maeda and Kurata 2011, Caicedo-Casso, Kang et al. 2015). In this case, we use multiparameter variations analysis to test the system robustness, as follows.

4.2.1 Parameters random perturbations analysis

To characterize system's robustness, it is important to estimate the changing rate of a target function with respect to changes in multiple parameters space caused by external factors such as temparature. Therefore, it is reasonable to perform random perturbation analysis of multiple parameters.

Before going to details of parameter perturbation analyses, it is worth describing how the parameter space for both the ACO and the RCO model was assigned. First, an extensive search was performed on the recruiting parameters that are responsible for maintaining oscillating behavior. Then, we selected an initial parameter set, which later re-scaled to conserve its oscillatory period approximately 24 hours. We search and select the default values in such a way that a small period variation could be seen if these default values are slightly varied while maintaining a 24-hour system's period. Finally, a parameter space mentioned in Table 1 was selected.

To evaluate the robustness of the phase difference, period and amplitude with respect to multiple parameter perturbations, we randomly varied the values of all the kinetic parameters by 10%, except a subset of the parameters (n, τ_1, τ_2, τ_3, τ_4, K_1, K_2) that are assumed insensitive to external fluctuations. More specificly, all the reaction rate kinetics embedded disturbances by following normal distributions with mean μ, and standard deviation σ;

$$\theta \sim N(\mu, \sigma) \qquad (4.1)$$

Where, θ represent the corresponding kinetic rate parameters in the system. μ is defined by as the symmetric kinetic set listed in Table 1 and σ is defined as $0.10\,\mu$.

In order to evaluate the robustness/ sensitivity, we iterelated this process 500 times to calculate the standard deviations (SDs) of the simulated phase differences, periods and

amplitudes. The SD was defined as the robustness of the oscillatory features to multi-parameter perturbations. A small SD indicates that its respective feature is robust to external perturbations.

4.3 Robustness to the molecular noise

Molecular noise, also known as intrinsic noise, is the expression variability that does not consider for by external noise, and typically originate from the interacting molecules of biochemical processes. (Gonze 2011, Singh and Soltani 2013). The circadian oscillator is defined as robust when the key features less strongly depend on the stochastic nature of the biochemical process, which controls the mechanism of the underlying molecular network.

When a system presented with a small number of interactive molecules, molecular noise may result in variations on the system's dynamics. Thus, stochasticity could limit or enhance certain behavioral features of systems of the circadian oscillators. In particular, stochasticity in the cellular level is responsible for limit the circadian clocks (Barkai and Leibler 2000). Another case, noise can improve some features of a biological system such as oscillatory behavior (Vilar, Kueh et al. 2002).

In this section, we investigate the robustness of both the ACO and the RCO models in measuring phase, period and amplitude by employing molecular noises. Intrinsic noise is implemented using the delayed stochastic simulation algorithm (DSSA). The DSSA is implemented through the MATLAB computer program, versions 2018a.

A detailed formulation of the stochastic model of the ACO/ RCO is given introduced in Chapter 3. Then, the molecular noise effects on the dynamics of the models is examined. To compute the mean period and amplitude, the Fast Fourier Transform (FFT) method was employed to the noisy output signals.

4.3.1 Stochastic simulation

Gillespie's stochastic simulation algorithm (SSA) is widely used for investigating the stochastic effects of genetic networks (Gillespie 1977, McAdams and Arkin 1997). The SSA is based on a Monte Carlo procedure, which accurately accounts for the inherent fluctuations and correlations that are not observed through a deterministic approach of the biochemical network. It is easy to program on a computer and offers a straightforward way to numerically estimate ensemble averages. But SSA is not able to deal with the explicit time delayed biochemical reaction process.

In this study, we employed the time-delay stochastic simulation algorithm (DSSA) developed by Barrio et al. (Barrio, Burrage et al. 2006, Zavala and Marquez-Lago 2014), which provides an exact sample path of the Markov chain model. The stochastic version of both the ACO and the RCO models have been discussed in Appendix-A, respectively.

Two hundred runs of the stochastic simulations were performed for different sets of coupling dissociation constant values (K_C) and time-delay (τ_c). A limitation of the DSSA is that it is not able to provide different time-delays to multiple reactions. It must set the unique time-delay in a simulation program.

4.3.2 Pseudo-code of the DSSA

INPUT DATA : Reactions defined by reactant and product vectors. Reactions are tagged as delayed or non-delayed. Stoichiometry. Reaction rates. Initial state X(0), Simulation time T. Delays

RESULT : State dynamics

PSEUDO-CODE :

```
begin
  t < T do
    generate r1 and r2 as U(0,1) random variables
    a0(X(t)) = sum{ j=1:m, aj(X(t))}
    θ = ln{1/r1 }/ a0(X(t))
    select j such that
        sum{k=1: j-1, ak (X(t))} < r2 * a0(X(t)) ≤ sum{k=1: j, ak (X(t))}

    if delayed reactions are scheduled within (t, t+θ) then
        let k be the delayed reaction scheduled next at time t+τ
          X(t+τ) = X(t) + Uk
          t = t + τ
    else
        if j is not delayed reaction then
          X(t+θ) = X(t) + Uj
          t = t + θ
    record time t + θ + τ for the delayed reaction
end
```

Figure 4.1 Delay Stochastic Simulation Algorithm (DSSA). DSSA is developed based on the reaction rejection method and accounts for distinct time delay reactions. In contrast to the Gillespie SSA, the DSSA makes explicit distinction between reaction waiting times (θ, in blue) and reaction delays (τ, in red). Pseudo-code reproduced from (Zavala and Marquez-Lago 2014).

4.4 Results

4.4.1 Robustness to multi-parameter random perturbations

We performed random parameter perurbation analyses to investigate the robustness of the symACO and symRCO models with respect to external perturbation and parameter uncertainty, as shown in Figure 4.2. In the phase transition regions, the SDs of the phase difference, period and amplitude in the ACO were higher than those in the RCO. Since the SD differences between the anti-phase ACO and in-phase RCO were not clearly illustrated in the non-transition regions, we added Figure S1 in the Appendix-B, to explicitly give the SD values. The SDs of phase difference and amplitude of the anti-phase ACO were larger than those of the in-phase RCO in the respective regions, while the period SDs of the anti-phase ACO were equal to or larger than those of the in-phase RCO. The ACO was found less robust than the RCO with respect to multi-parameter random perturbations.

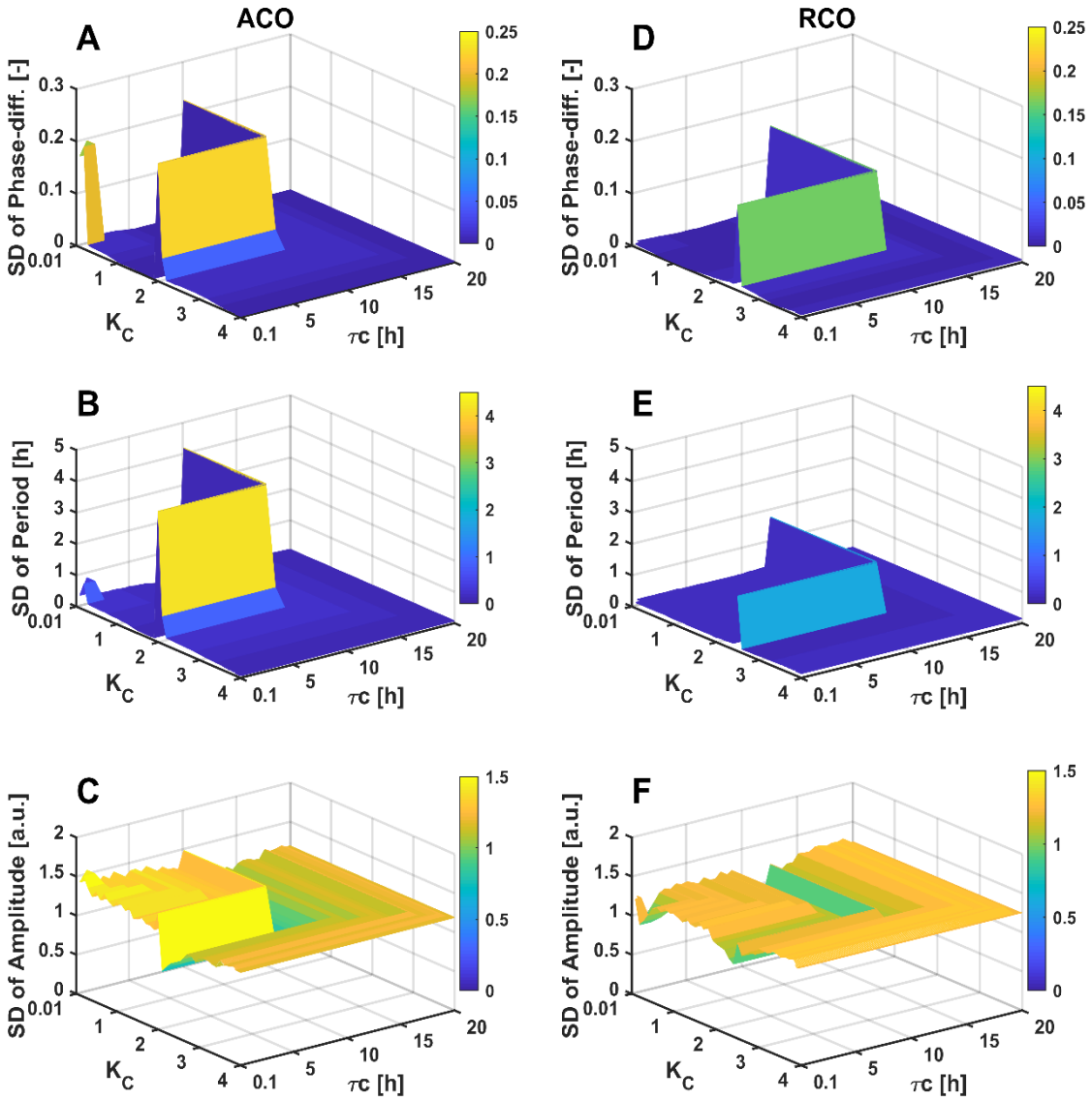

Figure 4.2. Robustness of the ACO and RCO under multi-parameter random perturbations. We recruited a different set of coupling dissociation constant (K_C) and coupling time-delay (τ_c). The employed kinetic parameters are listed in Table 3.1 of Chapter 3. The SDs are obtained from 500 runs of simulations. (A, B, C) The SDs of the phase difference, period, and amplitude were simulated for the symACO. (D, E, F) The SDs of the phase difference, period, and amplitude were simulated for the symRCO.

The multi-parameter random perturbation did not provide the symmetric kinetics to the two oscillators of the symACO at each simulation trial, due to the kinetic parameters being randomly selected, thus showing the anti-phase oscillators. In parameter uncertainty or random perturbations, the symACO definitely becomes the antiphse-oscillator.

4.4.2 Stochastic simulation

Biochemical reactions of circadian clocks are always exposed to stochastic noise (Gonze, Halloy et al. 2002, Gonze 2011, Gonze, Gérard et al. 2018). To investigate the effect of the stochasticity on both the symACO and symRCO, the DSSA was used to simulate the temporal patterns of the ACO and RCO, as shown in Figure 4.3. Two hundred runs of 10,000 hour stochastic simulations were performed with respect to K_C to calculate the mean period and amplitude. The ACO produced anti-phase oscillators (Figure 4.3A), whereas the RCO showed in-phase ones (Figure 4.3D). Interestingly, stochasticity changed the symACO to the anti-phase oscillator. It was unlikely for the ACO to show an in-phase oscillator in realistic, stochastic environments. Differing from the deterministic model of the in-phase symACO, the stochastic model of the symACO showed the antiphase oscillators, while increasing the amplitude with a decrease in *Kc*. The stochastic symACO no longer provides the in-phase oscillator, because the stochastic simulation never provides the perfect symmetric kinetics to the two oscillators of the ACO at each time point, although the kinetics of the two oscillators are symmetry on time average. The anti-phase oscillator of the symACO under stochastic noise is an interesting phenomenon that we have uncovered.

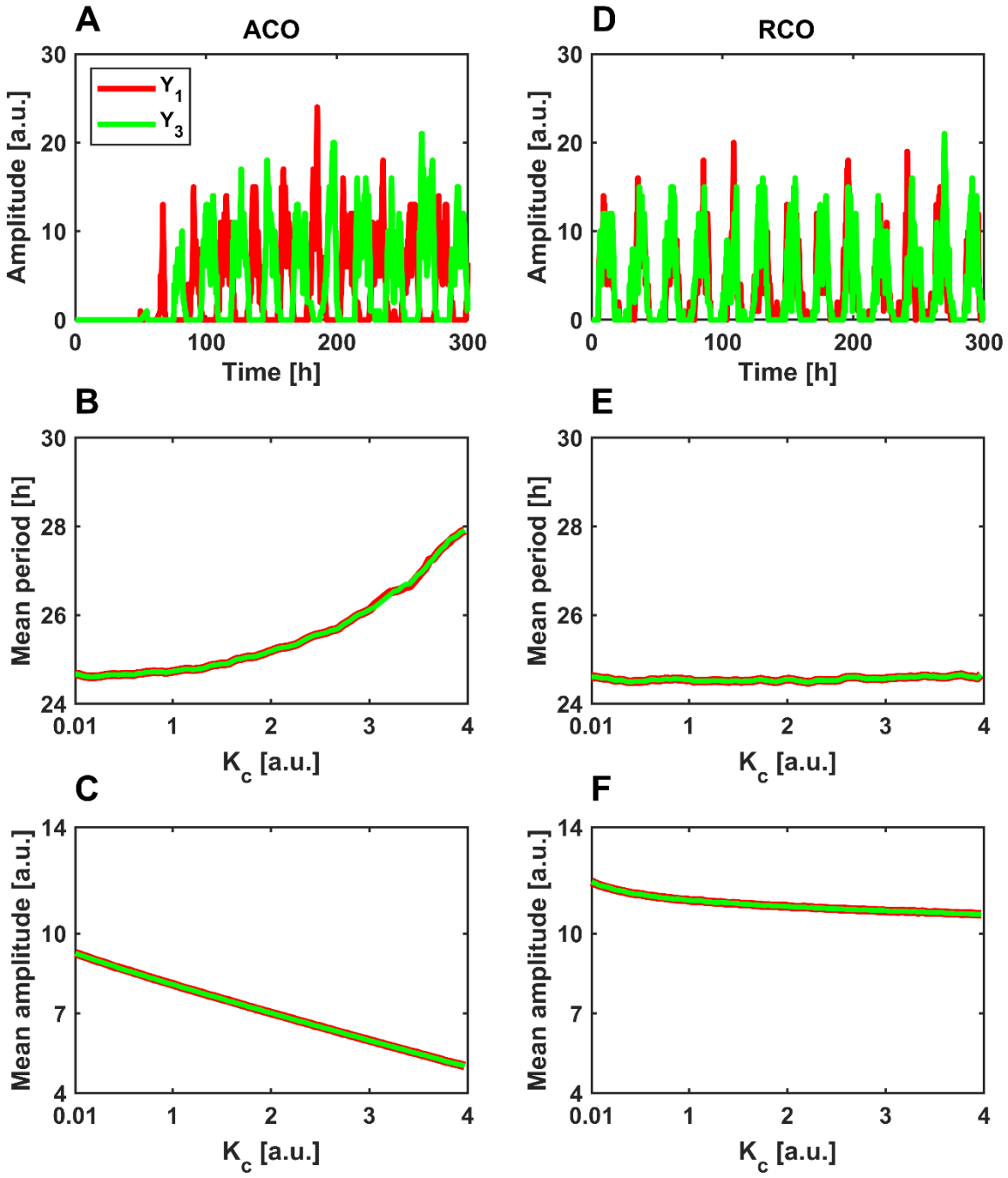

Figure 4.3. Stochastic simulation of ACO and RCO. The periods and amplitudes were averaged over 200 runs of stochastic simulations for the symACO and symRCO. We varied coupling dissociation constant (K_C), while fixing the other parameters, as shown in Table 3.1 of Chapter 3. (A) The time course of the ACO. (B, C) The mean periods and amplitudes of the ACO at different coupling dissociation constant (K_C). (D) The time course of the RCO.

E, F) The mean period and amplitude of the RCO at different coupling dissociation constant (K_C).

We evaluated the robustness of period and amplitude for both the stochastic models (Figure 4.3B, C, E, F). The mean period of the ACO was nearly 24 h in a range of K_C = 0.01-1.75, but the mean period increased with an increase in K_C at K_C >1.75. The mean amplitude gradually decreased with an increase in K_C. By contrast, the RCO provided almost constant periods of 24 h across a wide range of K_C. The amplitude of the RCO hardly decreased with an increase in K_C. The RCO produced robust period and amplitude compared to the ACO.

The periods of the ACO increased with an increase in K_C (Figure 4.3B). It is because the DSSA limitation constrains the multiple time-delays of the negative feedback oscillators $(\tau_1 = \tau_2 = \tau_3 = \tau_4)$ and coupling regulations $(\tau_c = \tau_5 = \tau_6)$, to be unique (Table 3.1 of Chapter 3). Thus, the stochastic results were not perfectly consistent with the deterministic ones, as shown in Figure S2 in Appendix-B. It shows the deterministic results of the phase differences, periods, and amplitudes of the ACO and RCO models employed by the stochastic analysis, where the multiple time-delays of the negative feedback oscillators and coupling regulations were set to be unique ($\tau_1 = \tau_2 = \tau_3 = \tau_4 = \tau_5 = \tau_6$). The stochastic analysis supported the deterministic results that a short coupling time-delay (approx. 5 h) made the ACO and RCO models anti-phase and in-phase oscillators (Figure 3.4A, D of Chapter 3), respectively. While both the ACO and RCO showed almost constant periods to a change in *K*c, the amplitude of the ACO were less robust than that of the RCO.

4.5 Discussion and conclusion

In this chapter, we investigate robustness of both the symACO and the symRCO models described in Chapter 3. We use the random parameter perturbations technique to measure robustness of the oscillation dynamics (phase, period and amplitude) with respect to the coupling dissociation constants (Kc, τ_c) to external noise (Figure 4.2). We also explore robustness of the stochastic ACO and the stochastic RCO models employing the distinct delayed stochastic simulation algorithms (DSSA) with respect to the coupling dissociation constants (Kc, τ_c) shown in Figure 4.3.

In stochastic environments, the symACO provided anti-phase oscillators (Figure 4.3A), differing from the deterministic result that the symACO showed an in-phase oscillator (Figure 3.2 of Chapter 3). In real, stochastic environment, the ACO was found to readily become anti-phase oscillators. The ACO indicated less robustness of period and amplitude with respect to the coupling dissociation constant, while the RCO produced in-phase oscillators that achieve almost constant period and amplitude regardless of the coupling dissociation constant. These stochastic results of the robustness were also consistent with those of the deterministic results.

In the multi-parameter random perturbation analysis and stochastic analysis, we did not employ the asymACO but symACO, while both the models showed almost the same results. The stochastic simulation of the symACO never provides the perfect symmetric kinetics to the two coupled oscillators at each time point, although the kinetics of the two oscillators are symmetry on time average. In the similar manner, the multi-parameter perturbation analysis did not provide the symmetric kinetics to the two oscillators at each simulation trial. We revealed that the symACO definitely turns to the anti-phase oscillator in realistic, stochastic environments and parameter uncertainty.

CHAPTER 5

ENTRAINABILITY OF THE COUPLED OSCILLATORS

Chapters 3 and 4 describe in details, how ACO and RCO models of the molecular circadian clock in *Drosophila* generate oscillations with 24-hour circadian period and how their circadian dynamics (phase, period and amplitude) change by the coupling dissociation constant. We also explore the effects of extrinsic and intrinsic noises by distinct random parameter perturbations and stochastic simulation analysis, with respect to the coupling dissociation constant (*Kc*, τ_c).

Here, we investigate the entrainment properties of both the ACO and the RCO models for the core circadian oscillator in the *Drosophila* system under different forcing (zeitgeber) cycles. Our results indicate that the coupling dissociation constant *Kc* is important to synchronize between the coupled oscillators of *Drosophila* to adapt to varying environmental cycles.

5.1 Master circadian clock, forcing period and entrainment

Many cellular and physiological activity controlled by the circadian clocks are temporally organized (Crosby, Hamnett et al. 2019). In a periodic environment circadian oscillators sense and make a precise respond to many photic (sunlight) and non-photic (temperature

and feeding) stimulus, to reliably function fulfil with a synchronized state (Bass and Takahashi 2010, Tahara and Shibata 2013, Hamaguchi, Tahara et al. 2015), even can persist in the absence of environmental input signals (Dubowy and Sehgal 2017). The circadian period between the circadian oscillator and the external force cycle is a key measure of the synchronized state (entrainment), which is required to invariantly adapt contributing the organism fitness. Using the system biology and experiment techniques a number of study intensively focus on the entrainment properties in several organisms including *Drosophila* (Dubowy and Sehgal 2017) and mammals (Gonze 2011).

Here, we investigate the entrainment of both the ACO and RCO models (chapter 3) for the circadian core oscillator in *Drosophila* under different zeitgeber forcing cycles. We show that coupled oscillators toward zeitgeber input can produce distinct entrainment ranges differing from 24h free running period with regarding a certain coupling dissociation parameter under different forcing cycle. Our study indicates that the coupling dissociation constant *Kc* between the coupled oscillators is critical and reveal the ACO model is less robust that the RCO model in synchronization state in *Drosophila* to varying environmental cycles.

The circadian clocks can function reliably under natural conditions if it invariantly stabilized or adjusted by external stimuli, including sunlight as "photic cues" and food, exercise, and temperature as "non-photic cues" (Bass and Takahashi 2010, Tahara and Shibata 2013). Although non-photic signals have the potential to entrain the circadian clocks, their influences have been masked with the photic stimuli (light) by considering as a strong synchronizer (zeitgeber). In figure 5.1, the entrainment scheme is displayed by the forcing cycle called master clock. The master clock influence/ activates the circadian

oscillators by differing the forcing cycle, then oscillators synchronized by the coupling forces to generate precise output rhythms.

5.2 Modeling zeitgeber input

Entrainment is known as the cornerstone of circadian clocks. The period is a key measure of entrainment. For a description of the circadian core oscillator in *Drosophila*, we use the two coupled oscillators the ACO and the RCO model described in chapter 3 with the given parameter set. In some organisms, like *Drosophila*, the exposure to light leads to increase degradation of the circadian clock protein TIM, which is known as the degradation response outlined in Figure 5.1 (Uriu and Tei 2019). Differently, in other organisms such as mammals (Shigeyoshi, Taguchi et al. 1997, Miyake, Sumi et al. 2000) and *Neurospora* (Crosthwaite, Loros et al. 1995, Crosthwaite, Dunlap et al. 1997), light signals induce the transcription of repressor mRNA.

In *Drosophila*, the transcription of '*per'* and '*tim'* genes are induced by the heterodimer transcription factor CLK /CYC (Figure 5.1). The *per*/*tim* mRNA (Y_1) is translated and accumulation the PER/TIM complex (Y_2). The PER/TIM heterodimer then represses the transcriptional activity of CLK/CYC (Y_4), forming a negative feedback loop (Tataroglu and Emery 2014). The CLK/CYC complex also activates transcription of the *vri* gene which inhibit the transcription of *Drosophila* Clock (*Clk*) gene. *Clk* mRNA (Y_3) is then translated by regulating the activation of CLK/CYC complex and complete the *Clk* feedback loop. Actually PER/TIM heterodimer indirectly activate the regulation of the CLK proteins (Allada 2003, Cyran, Buchsbaum et al. 2003, Glossop, Houl et al. 2003). By this core transcriptional-translational negative feedback loop, the abundance of TIM protein oscillates

under both LD and DD conditions (Myers, Wager-Smith et al. 1996, Zeng, Qian et al. 1996). Light signals activate *Cry* and it degrades TIM protein (Ceriani, Darlington et al. 1999, Naidoo, Song et al. 1999, Lin, Song et al. 2001, Koh, Zheng et al. 2006), which is independent from the natural degradation. This light-induced degradation of TIM allows the *Drosophila* clock to entrain to the LD cycle. As a result, the levels of TIM protein are lower during the day and higher during the night under LD conditions (Myers, Wager-Smith et al. 1996). Therefore, we model zeitgeber input by including an additional term in equation 3.1 and 3.5 of chapter 3 that allows the circadian clocks to entrain to the zeitgeber cycle regarded as the master clock. We assumed that the zeitgeber alters the degradation rate constant kd_1 of Y_1 (equation 3.1 and 3.5 described in Chapter 3) as follows:

$$kd_1 = kd_1 \times zeitgeber\ cycle \qquad (5.1)$$

The zeitgeber cycle was varied from 23 h to 32 h. Successful entrainment means that the period of oscillations is the same as the forcing period (less than 1% of deviation).

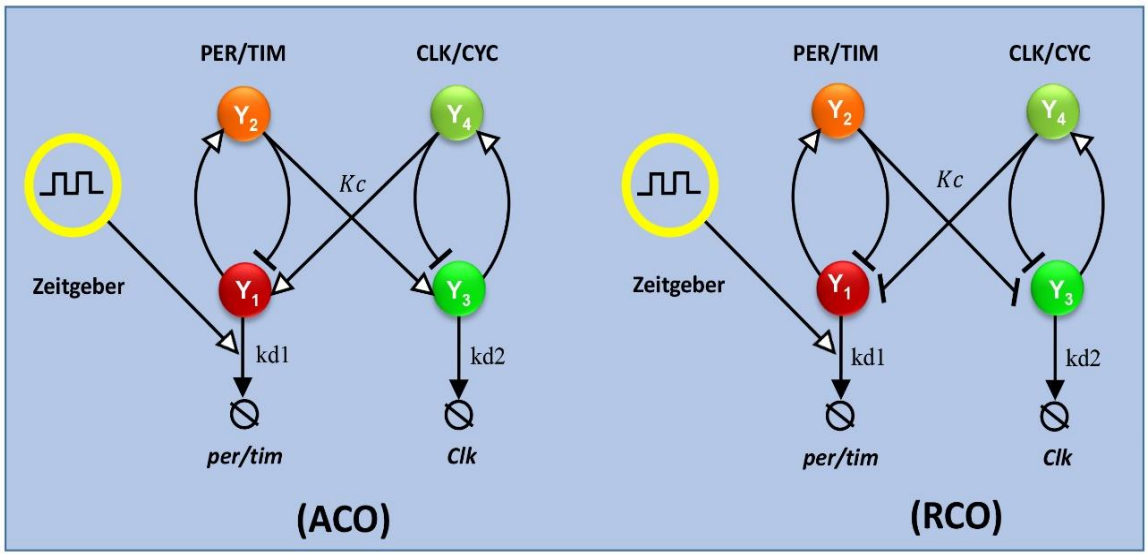

Figure 5.1. Scheme of the coupled feedback oscillators including zeitgeber (master clock) input. The transcription factor CLK/CYC (Y_4) promotes transcription of the *per* and *tim*

genes, which are treated as 1 variable. The *per*/*tim* mRNA (Y_1) is translated by accumulating PER/TIM complex (Y_2). The activated PER/TIM complex inhibits its own production by inhibiting CLK/CYC heterodimer and complete the *per*/*tim* negative feedback loop. The CLK/CYC (Y_4) complex also activates transcription of the *vri* gene which inhibit the transcription of *Clk* gene. *Clk* mRNA (Y_3) is then translated by regulating of CLK/CYC complex and complete the *Clk* feedback loop.

5.3 Results

Entrainment is the key cornerstone of circadian rhythms to adapt to the day-night cycle to control physiological and metabolic outputs at the right time (Hardin 2005). In analogy with the published work (Myers, Wager-Smith et al. 1996, Zeng, Qian et al. 1996), we investigate entrainability both of the asymACO and aymRCO under different forcing cycle. We altered a forcing period (master clock cycles) from 23 hours to 30 hours. In particular, we study the effect of coupling dissociation constant *Kc,* between the coupled oscillators on entrainment (synchronization) state (Figure 5.2).

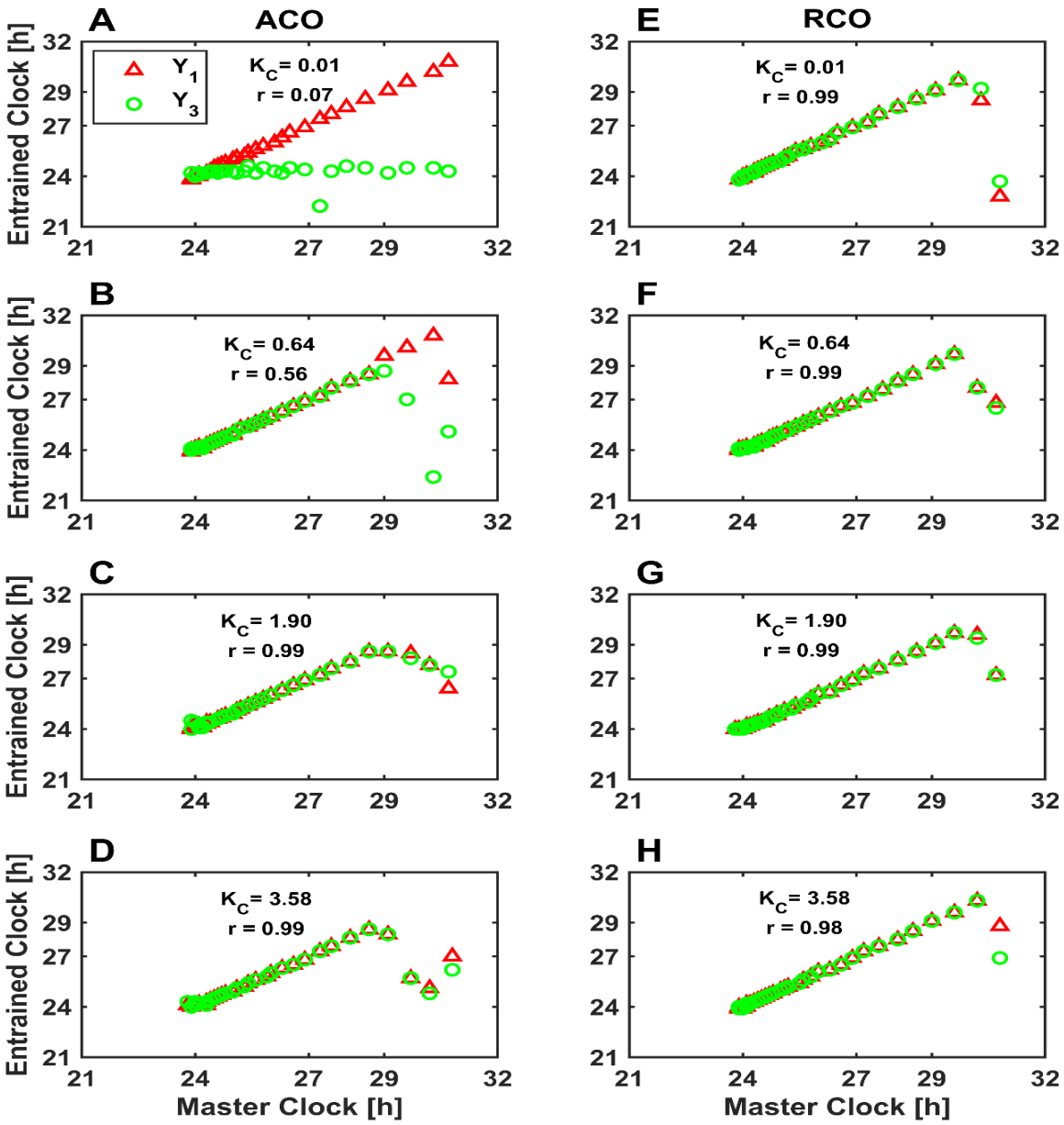

Figure 5.2. Entrainment analysis of the ACO and RCO. The periods of the entrained ACO and RCO were simulated with respect to the periods of the master clock. The asymACO and asymRCO were used. The employed parameters are shown in Table 3.1, of Chapter 3. Correlation between the two clocks is denoted by r. Red triangles mean Y_1 concentration; green circles Y_3. (A, B, C, D) Period relationships between the master clock and the entrained ACOs with a different value of K_C. (E, F, G, H) Period relationships between the master clock and the entrained RCOs with a different value of K_C.

As shown in Figure 5.2, at a very low dissociation constant of *Kc*, the Y_1 oscillator of the ACO was entrained by the master clock, but the Y_3 oscillator was not at all, or the Y_1 and Y_3 oscillators were not synchronized. With an increase in K_C, the Y_1 and Y_3 oscillators were interacted, then synchronized. The Y_3 oscillator was entrained by the master clock through the Y_1 oscillator. With a further increase in K_C, the Y_1 and Y_3 oscillators hardly entrained to the master clock with a period of 29 h. In the RCO, the Y_1 and Y_3 oscillators were synchronized in a region of K_C = 0.01-3.58. They were entrained by the master clock with a period of less than 30 hours, but were not with a period of 30 hours.

These results can be explained by considering the synchronization force between the Y_1 and Y_3 oscillators and the entrainment force between the Y_1 oscillator and the master clock. In the ACO, a very low value of K_C (= 0.01) indicates $\frac{Y_2}{K_C + Y_2} \rightarrow 1$ ($K_C << Y_2$). Since a change in Y_2 hardly affect Y_3, the synchronization force does not work. Consequently, the two oscillators within the ACO are hardly synchronized. With an increase in K_C, a change in Y_2 can effectively affect Y_3, strengthening the synchronization forces. At K_C greater than or equal to 1.90, the synchronization forces surpass the entrainment forces, thus the period of the Y_3 oscillator follows the Y_1 oscillator. The Y_1 and Y_3 oscillators entrain no longer to the master clock of a period of 29 hours. In the RCO, the Y_1 and Y_3 oscillators are synchronized in a region of K_C = 0.01-3.58, while the RCO entrains no longer to the master clock with a period of 30 hours. The RCO is found to enhance synchronization and entrainability with respect to K_C and a master clock period, compared to the ACO.

5.4 Conclusion

In this chapter, we performed entrainment analysis of both the asymACO and the asymRCO systems. We employed the master clock cycles as an external time giver (zeitgeber) as shown the schematic diagram in Figure 5.1. Entrainment has characterized by measuring one of the key circadian features oscillation period between the coupled oscillator and zeitgeber cycles.

Our finding importantly demonstrated that the ACO needed to finely adjust the coupling dissociation constant so that it can entrain to the environmental day-night cycle (Figure 5.2). The RCO produced higher entrainability across a wide range of the coupling dissociation constant than the ACO system. In the RCO system, the robust period and amplitude were simultaneously realized with high entrainability to day-night cycle. This result is consistent with some previous works that the robustness increases flexibility or entrainability (Akman, Rand et al. 2010, Maeda and Kurata 2012, Hatakeyama and Kaneko 2015).

CHAPTER 6

CONCLUSIONS AND FUTURE WORK

Circadian clocks simultaneously produce robust properties of period/amplitude and entrainability under external changes and stochastic fluctuations. This research is mainly aim to determine how the ACO evolves out of multiple interlocked feedback models that keep circadian time in *Drosophila melanogaster*. Although the interlocked feedback loops of the *per-tim* loop and *Clk* loop, the ACO, are known as typical structures, their design principles and molecular mechanism largely remain to be revealed. To solve this problem,

In Chapter 3, we first presented the ACO and RCO models (Figure 3.1). The ACO is a simplified model of existing interlocked feedback model; the RCO is a competitive, hypothetical model. We identified two key parameters: coupling dissociation constant, K_c and coupling time-delay, τ_c. By performing deterministic analyses, we show that both the symACO and symRCO provided in-phase oscillations (Figure 3.2), while the asymACO was changed to anti-phase oscillators (Figures 3.3 and 3.4), depending on coupling dissociation constant K_c and coupling time-delay τ_c. In contrast, the asymRCO presents the in-phase oscillator. These results indicated that the amplitude of the ACO was less robust than that of the RCO.

In Chapter 4, we devoted our effort to investigate the robustness of both the symACO and the symRCO models with respect to external and internal noises. We employed multi-parameter random perturbations analysis to characterize the influence of external noises by measuring SD values. Our finding indicated that the anti-phase ACO were less robust in the context of phase difference, period, and amplitude (Figure 4.2A, B, C) than those of the in-phase RCO in the respective regions (Figure 4.2D, E, F). In addition, in stochastic environments, the symACO provided anti-phase oscillators (Figure 4.3A), differing from the deterministic result that the symACO showed an in-phase oscillator (Figure 3.2). In real, stochastic environment, the ACO was found to readily become anti-phase oscillators. The ACO indicated less robustness of period and amplitude with respect to the coupling dissociation constant (Figure 4.3A, B, C), while the RCO produced in-phase oscillators that achieve almost constant period and amplitude regardless of the coupling dissociation constant (Figure 4.3D, E, F). These stochastic results of the robustness were also consistent with those of the deterministic results.

In the multi-parameter random perturbation analysis and stochastic analysis, we did not employ the asymACO but symACO, while both the models showed almost the same results. The stochastic simulation of the symACO never provides the perfect symmetric kinetics to the two coupled oscillators at each time point, although the kinetics of the two oscillators are symmetric on time average. In the similar manner, the multi-parameter perturbation analysis did not provide the symmetric kinetics to the two oscillators at each simulation trial. An interesting phenomenon that we first showed here is that the symACO definitely turns to the anti-phase oscillator into a realistic, stochastic environment and parameter uncertainty.

In Chapter 5, we examine the entrainability of both the asymACO and the asymRCO models with respect to the master clock (zeitgeber) cycles. In entrainment analysis, the ACO needed to finely adjust the coupling dissociation constant so that it can entrain to the environmental day-night cycle. The RCO produced higher entrainability across a wide range of the coupling dissociation constant than the ACO.

Smolen et. al (Smolen, Baxter et al. 2002) proposed an interlocked negative and positive feedback system, whose topology is similar to the ACO, to enhance the oscillation of the ACO over a single negative feedback loop, but did not consider any coupling protocols. Stelling et al. (Stelling, Gilles et al. 2004), and Maeda and Kurata (Maeda and Kurata 2012) constructed the hypothetical, redundant feedback model, whose structure was the same as the RCO, to demonstrate the enhanced robustness to its period/amplitude and entrainability, but did not compare it to the ACO. Those previous studies have not demonstrated any reason by which the coupling protocol of the ACO were selected instead of that of the RCO.

This study is the first to suggest here that how different coupling protocols of interlocked feedback loops, the ACO and RCO, generate characteristic functions of phase shift, robustness and entrainability. Considering that real circadian clocks evolve as the ACO, instead of the RCO, despite the reduced robustness of period and amplitude and less entrainability, we propose a novel hypothesis that the morning-evening, anti-phase cycle is more essential for *Drosophila* interlocked feedback loop than achieving the in-phase, robust, entrainable cycles.

In summary, we first demonstrated that in a real stochastic environment the ACO provides the anti-phase, fragile cycle; the RCO the in-phase, robust cycles with high entrainability. The ACO is less robust with respect to parameter uncertainty and stochasticity and less entrainable than the RCO, but the ACO has been selected or survived, suggesting the importance of the two antiphase clocks showing the peaks of the morning and evening activity, respectively (Stoleru, Peng et al. 2004). The morning and evening gene expression peaks are responsible for physiological events and behaviors, such as timing of the anabolic and catabolic functions (Sancar, Sancar et al. 2015), eclosion, courtship, the timing of rest and activity, locomotion (Tataroglu and Emery 2014, Franco, Frenkel et al. 2018), timing of feeding (Ro, Harvanek et al. 2014), and temperature preferences (Kaneko, Head et al. 2012), according to daily changes in environment. The two antiphase clocks are able to increase the variety of output time-courses by combining the two different peaks. It would be effective rather than the single (in-phase) clock in controlling many physiological functions according to complex environmental and internal cycles.

Finally, we illustrate some biological examples that couple intracellular feedback loops and inter-cellular signaling loops (Glossop, Houl et al. 2003, Gonze, Bernard et al. 2005, Soza-Ried, Öztürk et al. 2014, Battogtokh and Tyson 2018, Sonnen, Lauschke et al. 2018) as shown in Table 6.1. In segmentation clocks, adjacent cells/ inter-cellular feedback loops are combined to present anti-phase oscillators through protein signal transduction. In suprachiasmatic nucleus (SCN), inter-cellular feedback loops are coupled by mutual activation through neurotransmitters. In *Drosophila* and mammalian circadian clocks, intracellular oscillators are coupled mutually at gene expression level by activators. The ACO is widely used as the coupling protocol to combine two negative feedback loop.

A next step is to synthesize the ACO and RCO in microbes (e.g., *E. coli*) to demonstrate our mathematical model-based hypothesis. Since there are distinct functional differences in the phase shift within each coupled oscillator, we expect to uncover a design principle by which the ACO evolves in circadian clocks.

Bibliography

Abraham, U., A. E. Granada, P. O. Westermark, M. Heine, A. Kramer and H. Herzel (2010). "Coupling governs entrainment range of circadian clocks." Molecular systems biology **6**(1): 438.

Akman, O. E., D. A. Rand, P. E. Brown and A. J. Millar (2010). "Robustness from flexibility in the fungal circadian clock." BMC systems biology **4**(1): 88.

Allada, R. (2003). "Circadian clocks: a tale of two feedback loops." Cell **112**(3): 284-286.

Allada, R. and B. Y. Chung (2010). "Circadian organization of behavior and physiology in Drosophila." Annual review of physiology **72**: 605-624.

Allada, R., N. E. White, W. V. So, J. C. Hall and M. Rosbash (1998). "A mutant Drosophila homolog of mammalian Clock disrupts circadian rhythms and transcription of period and timeless." Cell **93**(5): 791-804.

Alon, U. (2019). An introduction to systems biology: design principles of biological circuits, CRC press.

Alves, R. and M. A. Savageau (2000). "Extending the method of mathematically controlled comparison to include numerical comparisons." Bioinformatics **16**(9): 786-798.

Amdaoud, M., M. Vallade, C. Weiss-Schaber and I. Mihalcescu (2007). "Cyanobacterial clock, a stable phase oscillator with negligible intercellular coupling." Proceedings of the National Academy of Sciences **104**(17): 7051-7056.

Aronson, B. D., K. A. Johnson, J. J. Loros and J. C. Dunlap (1994). "Negative feedback defining a circadian clock: autoregulation of the clock gene frequency." Science **263**(5153): 1578-1584.

Asgari-Targhi, A. and E. B. Klerman (2019). "Mathematical modeling of circadian rhythms." Wiley Interdisciplinary Reviews: Systems Biology and Medicine **11**(2): e1439.

Bae, K., C. Lee, D. Sidote, K. Y. Chuang and I. Edery (1998). "Circadian regulation of a Drosophila homolog of the mammalian Clock gene: PER and TIM function as positive regulators." Mol Cell Biol **18**(10): 6142-6151.

Bar-Even, A., J. Paulsson, N. Maheshri, M. Carmi, E. O'Shea, Y. Pilpel and N. Barkai (2006). "Noise in protein expression scales with natural protein abundance." Nature genetics **38**(6): 636-643.

Barkai, N. and S. Leibler (1997). "Robustness in simple biochemical networks." Nature **387**(6636): 913-917.

Barkai, N. and S. Leibler (2000). "Circadian clocks limited by noise." Nature **403**(6767): 267-268.

Barkai, N. and B.-Z. Shilo (2007). "Variability and robustness in biomolecular systems." Molecular cell **28**(5): 755-760.

Barrio, M., K. Burrage, A. Leier and T. Tian (2006). "Oscillatory regulation of Hes1: Discrete stochastic delay modelling and simulation." PLoS Comput Biol **2**(9): e117.

Bass, J. and J. S. Takahashi (2010). "Circadian integration of metabolism and energetics." Science **330**(6009): 1349-1354.

Battogtokh, D. and J. J. Tyson (2018). "Deciphering the Dynamics of Interlocked Feedback Loops in a Model of the Mammalian Circadian Clock." Biophysical journal **115**(10): 2055-2066.

Beersma, D. G. (2005). "Why and how do we model circadian rhythms?" Journal of biological rhythms **20**(4): 304-313.

Bhadra, U., N. Thakkar, P. Das and M. P. Bhadra (2017). "Evolution of circadian rhythms: from bacteria to human." Sleep medicine **35**: 49-61.

Bordyugov, G., U. Abraham, A. Granada, P. Rose, K. Imkeller, A. Kramer and H. Herzel (2015). "Tuning the phase of circadian entrainment." Journal of The Royal Society Interface **12**(108): 20150282.

Caicedo-Casso, A., H. W. Kang, S. Lim and C. I. Hong (2015). "Robustness and period sensitivity analysis of minimal models for biochemical oscillators." Sci Rep **5**: 13161.

Ceriani, M. F., T. K. Darlington, D. Staknis, P. Más, A. A. Petti, C. J. Weitz and S. A. Kay (1999). "Light-dependent sequestration of TIMELESS by CRYPTOCHROME." Science **285**(5427): 553-556.

Chaix, A., A. Zarrinpar, P. Miu and S. Panda (2014). "Time-restricted feeding is a preventative and therapeutic intervention against diverse nutritional challenges." Cell metabolism **20**(6): 991-1005.

Chang, D. C. and S. M. Reppert (2003). "A novel C-terminal domain of Drosophila PERIOD inhibits dCLOCK: CYCLE-mediated transcription." Current Biology **13**(9): 758-762.

Cheng, P., Y. Yang and Y. Liu (2001). "Interlocked feedback loops contribute to the robustness of the Neurospora circadian clock." Proc Natl Acad Sci U S A **98**(13): 7408-7413.

Chung, S., E. J. Lee, S. Yun, H. K. Choe, S.-B. Park, H. J. Son, K.-S. Kim, D. E. Dluzen, I. Lee and O. Hwang (2014). "Impact of circadian nuclear receptor REV-ERBα on midbrain dopamine production and mood regulation." Cell **157**(4): 858-868.

Crosby, P., R. Hamnett, M. Putker, N. P. Hoyle, M. Reed, C. J. Karam, E. S. Maywood, A. Stangherlin, J. E. Chesham and E. A. Hayter (2019). "Insulin/IGF-1 drives PERIOD synthesis to entrain circadian rhythms with feeding time." Cell **177**(4): 896-909. e820.

Crosthwaite, S. K., J. C. Dunlap and J. J. Loros (1997). "Neurospora wc-1 and wc-2: transcription, photoresponses, and the origins of circadian rhythmicity." Science **276**(5313): 763-769.

Crosthwaite, S. K., J. J. Loros and J. C. Dunlap (1995). "Light-induced resetting of a circadian clock is mediated by a rapid increase in frequency transcript." Cell **81**(7): 1003-1012.

Cummings, F. (1975). "A biochemical model of the circadian clock." Journal of theoretical biology **55**(2): 455-470.

Cyran, S. A., A. M. Buchsbaum, K. L. Reddy, M.-C. Lin, N. R. Glossop, P. E. Hardin, M. W. Young, R. V. Storti and J. Blau (2003). "vrille, Pdp1, and dClock form a second feedback loop in the Drosophila circadian clock." Cell **112**(3): 329-341.

Daan, S. and C. Berde (1978). "Two coupled oscillators: simulations of the circadian pacemaker in mammalian activity rhythms." Journal of Theoretical Biology **70**(3): 297-313.

Darlington, T. K., K. Wager-Smith, M. F. Ceriani, D. Staknis, N. Gekakis, T. D. Steeves, C. J. Weitz, J. S. Takahashi and S. A. Kay (1998). "Closing the circadian loop: CLOCK-induced transcription of its own inhibitors per and tim." Science **280**(5369): 1599-1603.

Dovzhenok, A. A., M. Baek, S. Lim and C. I. Hong (2015). "Mathematical modeling and validation of glucose compensation of the neurospora circadian clock." Biophysical journal **108**(7): 1830-1839.

Dubowy, C. and A. Sehgal (2017). "Circadian rhythms and sleep in Drosophila melanogaster." Genetics **205**(4): 1373-1397.

Fathallah-Shaykh, H. M., J. L. Bona and S. Kadener (2009). "Mathematical model of the Drosophila circadian clock: loop regulation and transcriptional integration." Biophys J **97**(9): 2399-2408.

Forger, D. B., M. E. Jewett and R. E. Kronauer (1999). "A simpler model of the human circadian pacemaker." Journal of biological rhythms **14**(6): 533-538.

Forger, D. B. and C. S. Peskin (2003). "A detailed predictive model of the mammalian circadian clock." Proceedings of the National Academy of Sciences **100**(25): 14806-14811.

Franco, D. L., L. Frenkel and M. F. Ceriani (2018). "The underlying genetics of drosophila circadian behaviors." Physiology **33**(1): 50-62.

Gardner, T. S., C. R. Cantor and J. J. Collins (2000). "Construction of a genetic toggle switch in Escherichia coli." Nature **403**(6767): 339.

Gekakis, N., L. Saez, A.-M. Delahaye-Brown, M. P. Myers, A. Sehgal, M. W. Young and C. J. Weitz (1995). "Isolation of timeless by PER protein interaction: defective interaction between timeless protein and long-period mutant PERL." Science **270**(5237): 811-815.

Gillespie, D. T. (1977). "Exact stochastic simulation of coupled chemical reactions." The Journal of Physical Chemistry **81**(25): 2340-2361.

Gillespie, D. T. (2007). "Stochastic simulation of chemical kinetics." Annu. Rev. Phys. Chem. **58**: 35-55.

Glossop, N. R., J. H. Houl, H. Zheng, F. S. Ng, S. M. Dudek and P. E. Hardin (2003). "VRILLE feeds back to control circadian transcription of Clock in the Drosophila circadian oscillator." Neuron **37**(2): 249-261.

Glossop, N. R., L. C. Lyons and P. E. Hardin (1999). "Interlocked feedback loops within the Drosophila circadian oscillator." Science **286**(5440): 766-768.

Gonze, D. (2011). "Modeling circadian clocks: From equations to oscillations." Central European Journal of Biology **6**(5): 699.

Gonze, D. (2011). "Modeling circadian clocks: roles, advantages, and limitations." Open Life Sciences **6**(5): 712-729.

Gonze, D., S. Bernard, C. Waltermann, A. Kramer and H. Herzel (2005). "Spontaneous synchronization of coupled circadian oscillators." Biophys J **89**(1): 120-129.

Gonze, D., C. Gérard, B. Wacquier, A. Woller, A. Tosenberger, A. Goldbeter and G. Dupont (2018). "Modeling-based investigation of the effect of noise in cellular systems." Frontiers in Molecular Biosciences **5**: 34.

Gonze, D., J. Halloy and A. Goldbeter (2002). "Robustness of circadian rhythms with respect to molecular noise." Proceedings of the National Academy of Sciences of the United States of America **99**(2): 673-678.

Gonze, D., M. R. Roussel and A. Goldbeter (2002). "A model for the enhancement of fitness in cyanobacteria based on resonance of a circadian oscillator with the external light–dark cycle." Journal of theoretical biology **214**(4): 577-597.

Goodwin, B. C. (1965). "Oscillatory behavior in enzymatic control processes." Advances in enzyme regulation **3**: 425-437.

Goodwin, B. C. (1997). "Temporal organization and disorganization in organisms." Chronobiology international **14**(5): 531-536.

Granada, A. E. and H. Herzel (2009). "How to achieve fast entrainment? The timescale to synchronization." PloS one **4**(9).

Griffith, J. S. (1968). "Mathematics of cellular control processes. I. Negative feedback to one gene." J Theor Biol **20**(2): 202-208.

Hafner, M., H. Koeppl, M. Hasler and A. Wagner (2009). "'Glocal' robustness analysis and model discrimination for circadian oscillators." PLoS Comput Biol **5**(10): e1000534.

Hamaguchi, Y., Y. Tahara, H. Kuroda, A. Haraguchi and S. Shibata (2015). "Entrainment of mouse peripheral circadian clocks to< 24 h feeding/fasting cycles under 24 h light/dark conditions." Scientific reports **5**: 14207.

Hardin, P. E. (2005). "The circadian timekeeping system of Drosophila." Curr Biol **15**(17): R714-722.

Hardin, P. E. (2011). Molecular genetic analysis of circadian timekeeping in Drosophila. Advances in genetics, Elsevier. **74:** 141-173.

Hardin, P. E., J. C. Hall and M. Rosbash (1990). "Feedback of the Drosophila period gene product on circadian cycling of its messenger RNA levels." Nature **343**(6258): 536.

Hasan, A. S. U. and H. Kurata (2017). "Mathematical comparison of memory functions between mutual activation and repression networks in a stochastic environment." Journal of theoretical biology **427**: 28-40.

Hatakeyama, T. S. and K. Kaneko (2015). "Reciprocity Between Robustness of Period and Plasticity of Phase in Biological Clocks." Physical Review Letters **115**(21): 218101.

Hilfinger, A. and J. Paulsson (2011). "Separating intrinsic from extrinsic fluctuations in dynamic biological systems." Proceedings of the National Academy of Sciences **108**(29): 12167-12172.

Jagannath, A., L. Taylor, Z. Wakaf, S. R. Vasudevan and R. G. Foster (2017). "The genetics of circadian rhythms, sleep and health." Human molecular genetics **26**(R2): R128-R138.

Kaern, M., T. C. Elston, W. J. Blake and J. J. Collins (2005). "Stochasticity in gene expression: from theories to phenotypes." Nat Rev Genet **6**(6): 451-464.

Kaneko, H., L. M. Head, J. Ling, X. Tang, Y. Liu, P. E. Hardin, P. Emery and F. N. Hamada (2012). "Circadian rhythm of temperature preference and its neural control in Drosophila." Current Biology **22**(19): 1851-1857.

Kay, S. K., H. A. Harrington, S. Shepherd, K. Brennan, T. Dale, J. M. Osborne, D. J. Gavaghan and H. M. Byrne (2017). "The role of the Hes1 crosstalk hub in Notch-Wnt interactions of the intestinal crypt." PLoS computational biology **13**(2): e1005400.

Kidd, P. B., M. W. Young and E. D. Siggia (2015). "Temperature compensation and temperature sensation in the circadian clock." Proceedings of the National Academy of Sciences **112**(46): E6284-E6292.

Kim, J. K. and D. B. Forger (2012). "A mechanism for robust circadian timekeeping via stoichiometric balance." Molecular systems biology **8**(1).

Kim, J. R., D. Shin, S. H. Jung, P. Heslop-Harrison and K. H. Cho (2010). "A design principle underlying the synchronization of oscillations in cellular systems." J Cell Sci **123**(Pt 4): 537-543.

Klotter, K. (1960). Theoretical analysis of some biological models. Cold Spring Harbor symposia on quantitative biology, Cold Spring Harbor Laboratory Press.

Ko, C. H. and J. S. Takahashi (2006). "Molecular components of the mammalian circadian clock." Human Molecular Genetics **15**(suppl_2): R271-R277.

Koh, K., X. Zheng and A. Sehgal (2006). "JETLAG resets the Drosophila circadian clock by promoting light-induced degradation of TIMELESS." Science **312**(5781): 1809-1812.

Komin, N., A. C. Murza, E. Hernández-García and R. Toral (2010). "Synchronization and entrainment of coupled circadian oscillators." Interface focus **1**(1): 167-176.

Kunz, H. and P. Achermann (2003). "Simulation of circadian rhythm generation in the suprachiasmatic nucleus with locally coupled self-sustained oscillators." Journal of theoretical biology **224**(1): 63-78.

Kurata, H., T. Tanaka and F. Ohnishi (2007). "Mathematical identification of critical reactions in the interlocked feedback model." PLoS One **2**(10): e1103.

Kurosawa, G., A. Mochizuki and Y. Iwasa (2002). "Comparative study of circadian clock models, in search of processes promoting oscillation." J Theor Biol **216**(2): 193-208.

Leise, T. L. and E. E. Moin (2007). "A mathematical model of the Drosophila circadian clock with emphasis on posttranslational mechanisms." Journal of theoretical biology **248**(1): 48-63.

Leloup, J.-C. and A. Goldbeter (1997). "Temperature compensation of circadian rhythms: control of the period in a model for circadian oscillations of the per protein in Drosophila." Chronobiology international **14**(5): 511-520.

Leloup, J.-C. and A. Goldbeter (2003). "Toward a detailed computational model for the mammalian circadian clock." Proceedings of the National Academy of Sciences **100**(12): 7051-7056.

Leloup, J. C. and A. Goldbeter (1998). "A model for circadian rhythms in Drosophila incorporating the formation of a complex between the PER and TIM proteins." J Biol Rhythms **13**(1): 70-87.

Lema, M. A., D. A. Golombek and J. Echave (2000). "Delay model of the circadian pacemaker." Journal of theoretical biology **204**(4): 565-573.

Lewis, J. (2003). "Autoinhibition with transcriptional delay: a simple mechanism for the zebrafish somitogenesis oscillator." Current Biology **13**(16): 1398-1408.

Lin, F.-J., W. Song, E. Meyer-Bernstein, N. Naidoo and A. Sehgal (2001). "Photic Signaling by Cryptochrome in the DrosophilaCircadian System." Molecular and cellular biology **21**(21): 7287-7294.

Locke, J. C., L. Kozma-Bognár, P. D. Gould, B. Fehér, E. Kevei, F. Nagy, M. S. Turner, A. Hall and A. J. Millar (2006). "Experimental validation of a predicted feedback loop in the multi-oscillator clock of Arabidopsis thaliana." Molecular systems biology **2**(1).

Locke, J. C., A. J. Millar and M. S. Turner (2005). "Modelling genetic networks with noisy and varied experimental data: the circadian clock in Arabidopsis thaliana." J Theor Biol **234**(3): 383-393.

Lowrey, P. L. and J. S. Takahashi (2011). Genetics of circadian rhythms in Mammalian model organisms. Advances in genetics, Elsevier. **74:** 175-230.

Maeda, K. and H. Kurata (2011). "Quasi-multiparameter sensitivity measure for robustness analysis of complex biochemical networks." Journal of theoretical biology **272**(1): 174-186.

Maeda, K. and H. Kurata (2012). "A symmetric dual feedback system provides a robust and entrainable oscillator." PloS one **7**(2): e30489.

McAdams, H. H. and A. Arkin (1997). "Stochastic mechanisms in gene expression." Proc Natl Acad Sci U S A **94**(3): 814-819.

Miyake, S., Y. Sumi, L. Yan, S. Takekida, T. Fukuyama, Y. Ishida, S. Yamaguchi, K. Yagita and H. Okamura (2000). "Phase-dependent responses of Per1 and Per2 genes to a light-stimulus in the suprachiasmatic nucleus of the rat." Neuroscience letters **294**(1): 41-44.

Munsky, B., G. Neuert and A. Van Oudenaarden (2012). "Using gene expression noise to understand gene regulation." Science **336**(6078): 183-187.

Myers, M. P., K. Wager-Smith, A. Rothenfluh-Hilfiker and M. W. Young (1996). "Light-induced degradation of TIMELESS and entrainment of the Drosophila circadian clock." Science **271**(5256): 1736-1740.

Naidoo, N., W. Song, M. Hunter-Ensor and A. Sehgal (1999). "A role for the proteasome in the light response of the timeless clock protein." Science **285**(5434): 1737-1741.

Novák, B. and J. J. Tyson (2008). "Design principles of biochemical oscillators." Nature reviews Molecular cell biology **9**(12): 981-991.

olde Scheper, T., D. Klinkenberg, C. Pennartz and J. Van Pelt (1999). "A mathematical model for the intracellular circadian rhythm generator." Journal of Neuroscience **19**(1): 40-47.

Ozbudak, E. M., M. Thattai, I. Kurtser, A. D. Grossman and A. Van Oudenaarden (2002). "Regulation of noise in the expression of a single gene." Nature genetics **31**(1): 69-73.

Patke, A., M. W. Young and S. Axelrod (2019). "Molecular mechanisms and physiological importance of circadian rhythms." Nature Reviews Molecular Cell Biology: 1-18.

Pavlidis, T. (1967). "A model for circadian clocks." The bulletin of mathematical biophysics **29**(4): 781-791.

Pavlidis, T. and W. Kauzmann (1969). "Toward a quantitative biochemical model for circadian oscillators." Archives of biochemistry and biophysics **132**(1): 338-348.

Pfeuty, B., Q. Thommen and M. Lefranc (2011). "Robust entrainment of circadian oscillators requires specific phase response curves." Biophysical journal **100**(11): 2557-2565.

Putker, M., P. Crosby, K. A. Feeney, N. P. Hoyle, A. S. Costa, E. Gaude, C. Frezza and J. S. O'Neill (2018). "Mammalian circadian period, but not phase and amplitude, is robust against redox and metabolic perturbations." Antioxidants & redox signaling **28**(7): 507-520.

Rand, D., B. Shulgin, J. Salazar and A. Millar (2006). "Uncovering the design principles of circadian clocks: mathematical analysis of flexibility and evolutionary goals." Journal of Theoretical Biology **238**(3): 616-635.

Relógio, A., P. O. Westermark, T. Wallach, K. Schellenberg, A. Kramer and H. Herzel (2011). "Tuning the mammalian circadian clock: robust synergy of two loops." PLoS computational biology **7**(12).

Rendon, D., V. Walton, G. Tait, J. Buser, I. Lemos Souza, A. Wallingford, G. Loeb and J. Lee (2019). "Interactions among morphotype, nutrition, and temperature impact fitness of an invasive fly." Ecology and evolution **9**(5): 2615-2628.

Richards, J. and M. L. Gumz (2013). "Mechanism of the circadian clock in physiology." American Journal of Physiology-Regulatory, Integrative and Comparative Physiology **304**(12): R1053-R1064.

Ro, J., Z. M. Harvanek and S. D. Pletcher (2014). "FLIC: high-throughput, continuous analysis of feeding behaviors in Drosophila." PloS one **9**(6).

Roenneberg, T., Z. Dragovic and M. Merrow (2005). "Demasking biological oscillators: properties and principles of entrainment exemplified by the Neurospora circadian clock." Proceedings of the National Academy of Sciences **102**(21): 7742-7747.

Rougemont, J. and F. Naef (2006). "Collective synchronization in populations of globally coupled phase oscillators with drifting frequencies." Physical Review E **73**(1): 011104.

Ruoff, P., M. K. Christensen and V. K. Sharma (2005). "PER/TIM-mediated amplification, gene dosage effects and temperature compensation in an interlocking-feedback loop model of the Drosophila circadian clock." Journal of theoretical biology **237**(1): 41-57.

Ruoff, P., J. J. Loros and J. C. Dunlap (2005). "The relationship between FRQ-protein stability and temperature compensation in the Neurospora circadian clock." Proceedings of the National Academy of Sciences **102**(49): 17681-17686.

Ruoff, P. and L. Rensing (1996). "The temperature-compensated Goodwin model simulates many circadian clock properties." Journal of Theoretical Biology **179**(4): 275-285.

Ruoff, P., M. Vinsjevik, C. Monnerjahn and L. Rensing (1999). "The Goodwin oscillator: on the importance of degradation reactions in the circadian clock." Journal of biological rhythms **14**(6): 469-479.

Rutila, J. E., V. Suri, M. Le, W. V. So, M. Rosbash and J. C. Hall (1998). "CYCLE is a second bHLH-PAS clock protein essential for circadian rhythmicity and transcription of Drosophila period and timeless." Cell **93**(5): 805-814.

Sancar, C., G. Sancar, N. Ha, F. Cesbron and M. Brunner (2015). "Dawn-and dusk-phased circadian transcription rhythms coordinate anabolic and catabolic functions in Neurospora." BMC biology **13**(1): 17.

Shigeyoshi, Y., K. Taguchi, S. Yamamoto, S. Takekida, L. Yan, H. Tei, T. Moriya, S. Shibata, J. J. Loros and J. C. Dunlap (1997). "Light-induced resetting of a mammalian circadian clock is associated with rapid induction of the mPer1 transcript." Cell **91**(7): 1043-1053.

Shimojo, H., A. Isomura, T. Ohtsuka, H. Kori, H. Miyachi and R. Kageyama (2016). "Oscillatory control of Delta-like1 in cell interactions regulates dynamic gene expression and tissue morphogenesis." Genes & development **30**(1): 102-116.

Singh, A. and M. Soltani (2013). "Quantifying intrinsic and extrinsic variability in stochastic gene expression models." Plos one **8**(12).

Smolen, P., D. A. Baxter and J. H. Byrne (2001). "Modeling circadian oscillations with interlocking positive and negative feedback loops." J Neurosci **21**(17): 6644-6656.

Smolen, P., D. A. Baxter and J. H. Byrne (2002). "A reduced model clarifies the role of feedback loops and time delays in the Drosophila circadian oscillator." Biophys J **83**(5): 2349-2359.

Smolen, P., P. E. Hardin, B. S. Lo, D. A. Baxter and J. H. Byrne (2004). "Simulation of Drosophila circadian oscillations, mutations, and light responses by a model with VRI, PDP-1, and CLK." Biophys J **86**(5): 2786-2802.

Sonnen, K. F., V. M. Lauschke, J. Uraji, H. J. Falk, Y. Petersen, M. C. Funk, M. Beaupeux, P. François, C. A. Merten and A. Aulehla (2018). "Modulation of phase shift between Wnt and Notch signaling oscillations controls mesoderm segmentation." Cell **172**(5): 1079-1090. e1012.

Soza-Ried, C., E. Öztürk, D. Ish-Horowicz and J. Lewis (2014). "Pulses of Notch activation synchronise oscillating somite cells and entrain the zebrafish segmentation clock." Development **141**(8): 1780-1788.

Sriram, K. and M. Gopinathan (2004). "A two variable delay model for the circadian rhythm of Neurospora crassa." Journal of theoretical biology **231**(1): 23-38.

Stelling, J., E. D. Gilles and F. J. Doyle, 3rd (2004). "Robustness properties of circadian clock architectures." Proc Natl Acad Sci U S A **101**(36): 13210-13215.

Stoleru, D., Y. Peng, J. Agosto and M. Rosbash (2004). "Coupled oscillators control morning and evening locomotor behaviour of Drosophila." Nature **431**(7010): 862-868.

Swain, P. S., M. B. Elowitz and E. D. Siggia (2002). "Intrinsic and extrinsic contributions to stochasticity in gene expression." Proceedings of the National Academy of Sciences **99**(20): 12795-12800.

Tahara, Y. and S. Shibata (2013). "Chronobiology and nutrition." Neuroscience **253**: 78-88.

Takeuchi, T., T. Hinohara, G. Kurosawa and K. Uchida (2007). "A temperature-compensated model for circadian rhythms that can be entrained by temperature cycles." Journal of theoretical biology **246**(1): 195-204.

Tataroglu, O. and P. Emery (2014). "Studying circadian rhythms in Drosophila melanogaster." Methods **68**(1): 140-150.

Tsai, T. Y.-C., Y. S. Choi, W. Ma, J. R. Pomerening, C. Tang and J. E. Ferrell (2008). "Robust, tunable biological oscillations from interlinked positive and negative feedback loops." Science **321**(5885): 126-129.

Tyson, J. J. (2002). Biochemical oscillations. Computational cell biology, Springer**:** 230-260.

Ueda, H. R., M. Hagiwara and H. Kitano (2001). "Robust oscillations within the interlocked feedback model of Drosophila circadian rhythm." J Theor Biol **210**(4): 401-406.

Uriu, K. and L. G. Morelli (2017). "Determining the impact of cell mixing on signaling during development." Development, growth & differentiation **59**(5): 351-368.

Uriu, K. and H. Tei (2019). "A saturated reaction in repressor synthesis creates a daytime dead zone in circadian clocks." PLoS computational biology **15**(2): e1006787.

Van der Pol, B. (1960). A theory of the amplitude of free and forced triode vibrations, Radio Rev. 1 (1920) 701-710, 754-762; Selected Scientific Papers, vol. I, North Holland.

Vilar, J. M., H. Y. Kueh, N. Barkai and S. Leibler (2002). "Mechanisms of noise-resistance in genetic oscillators." Proceedings of the National Academy of Sciences **99**(9): 5988-5992.

Wagner, A. (2005). "Circuit topology and the evolution of robustness in two-gene circadian oscillators." Proceedings of the National Academy of Sciences **102**(33): 11775-11780.

Williams, C. M., M. D. McCue, N. E. Sunny, A. Szejner-Sigal, T. J. Morgan, D. B. Allison and D. A. Hahn (2016). "Cold adaptation increases rates of nutrient flow and metabolic plasticity during cold exposure in Drosophila melanogaster." Proceedings of the Royal Society B: Biological Sciences **283**(1838): 20161317.

Wolf, J., S. Becker-Weimann and R. Heinrich (2005). "Analysing the robustness of cellular rhythms." Systems biology **2**(1): 35-41.

Xie, Z. and D. Kulasiri (2007). "Modelling of circadian rhythms in Drosophila incorporating the interlocked PER/TIM and VRI/PDP1 feedback loops." J Theor Biol **245**(2): 290-304.

Xu, Y., K. Toh, C. Jones, J.-Y. Shin, Y.-H. Fu and L. Ptáček (2007). "Modeling of a human circadian mutation yields insights into clock regulation by PER2." Cell **128**(1): 59-70.

Yan, J., G. Shi, Z. Zhang, X. Wu, Z. Liu, L. Xing, Z. Qu, Z. Dong, L. Yang and Y. Xu (2014). "An intensity ratio of interlocking loops determines circadian period length." Nucleic acids research **42**(16): 10278-10287.

Yang, Q., B. F. Pando, G. Dong, S. S. Golden and A. van Oudenaarden (2010). "Circadian gating of the cell cycle revealed in single cyanobacterial cells." Science **327**(5972): 1522-1526.

Yu, W., H. Zheng, J. L. Price and P. E. Hardin (2009). "DOUBLETIME plays a noncatalytic role to mediate CLOCK phosphorylation and repress CLOCK-dependent transcription within the Drosophila circadian clock." Molecular and cellular biology **29**(6): 1452-1458.

Zavala, E. and T. T. Marquez-Lago (2014). "Delays induce novel stochastic effects in negative feedback gene circuits." Biophys J **106**(2): 467-478.

Zeng, H., Z. Qian, M. P. Myers and M. Rosbash (1996). "A light-entrainment mechanism for the Drosophila circadian clock." Nature **380**(6570): 129-135.

Zhang, R., N. F. Lahens, H. I. Ballance, M. E. Hughes and J. B. Hogenesch (2014). "A circadian gene expression atlas in mammals: implications for biology and medicine." Proceedings of the National Academy of Sciences **111**(45): 16219-16224.

Appendix- A

Table 4.1: **Stochastic version of the ACO model**

Reaction Number	Reaction	Propensity of Reaction	Transition
1	$\Phi \rightarrow Y_1 + \Phi$	$a_1 = b_1 + k_1 \frac{K_1^{\,n}}{K_1^{\,n} + Y_2(t-\tau_2)^n} \frac{Y_4(t-\tau_5)}{K_3 + Y_4(t-\tau_5)}$	$Y_1 \rightarrow Y_1 + 1$
2	$Y_1 \rightarrow \phi$	$a_2 = kd_1 Y_1$	$Y_1 \rightarrow Y_1 - 1$
3	$Y_1 \rightarrow Y_2$	$a_3 = Y_1(t-\tau_1)$	$Y_2 \rightarrow Y_2 + 1$
4	$Y_2 \rightarrow \phi$	$a_4 = Y_2$	$Y_2 \rightarrow Y_2 - 1$
5	$\Phi \rightarrow Y_3 + \Phi$	$a_5 = b_2 + k_2 \frac{K_2^{\,n}}{K_2^{\,n} + Y_4(t-\tau_4)^n} \frac{Y_2(t-\tau_6)}{K_4 + Y_2(t-\tau_6)}$	$Y_3 \rightarrow Y_3 + 1$
6	$Y_3 \rightarrow \phi$	$a_6 = kd_2 Y_3$	$Y_3 \rightarrow Y_3 - 1$
7	$Y_3 \rightarrow Y_4$	$a_7 = Y_3(t-\tau_3)$	$Y_4 \rightarrow Y_4 + 1$
8	$Y_4 \rightarrow \phi$	$a_8 = Y_4$	$Y_4 \rightarrow Y_4 - 1$

This table lists the sequence of reactions corresponding to the chemical network of the ACO governed by the ODE system (equations 3.1-3.4). The second column lists the sequence of reactions. The third column shows the propensity function associated with each reaction. The last column indicates the change in number of molecules of each species depending on the different reactions. The symbol ϕ indicates a degradation process. Φ represents the gene that transcribes mRNA.

Table 4.2: **Stochastic version of the RCO model**

Reaction Number	Reaction	Propensity of Reaction	Transition
1	$\Phi \rightarrow Y_1 + \Phi$	$a_1 = b_1 + k_1 \frac{K_1^{\,n}}{K_1^{\,n} + Y_2(t-\tau_2)^n} \frac{K_3}{K_3 + Y_4(t-\tau_5)}$	$Y_1 \rightarrow Y_1 + 1$
2	$Y_1 \rightarrow \phi$	$a_2 = kd_1 Y_1$	$Y_1 \rightarrow Y_1 - 1$
3	$Y_1 \rightarrow Y_2$	$a_3 = Y_1(t-\tau_1)$	$Y_2 \rightarrow Y_2 + 1$
4	$Y_2 \rightarrow \phi$	$a_4 = Y_2$	$Y_2 \rightarrow Y_2 - 1$
5	$\Phi \rightarrow Y_3 + \Phi$	$a_5 = b_2 + k_2 \frac{K_2^{\,n}}{K_2^{\,n} + Y_4(t-\tau_4)^n} \frac{K_4}{K_4 + Y_2(t-\tau_6)}$	$Y_3 \rightarrow Y_3 + 1$
6	$Y_3 \rightarrow \phi$	$a_6 = kd_2 Y_3$	$Y_3 \rightarrow Y_3 - 1$
7	$Y_3 \rightarrow Y_4$	$a_7 = Y_3(t-\tau_3)$	$Y_4 \rightarrow Y_4 + 1$
8	$Y_4 \rightarrow \phi$	$a_8 = Y_4$	$Y_4 \rightarrow Y_4 - 1$

This table lists the sequence of reactions corresponding to the chemical network of the ACO governed by the ODE system (equations 3.5-3.8). The second column lists the sequence of reactions. The third column shows the propensity function associated with each reaction. The last column indicates the change in number of molecules of each species depending on the different reactions. The symbol ϕ indicates a degradation process. Φ represents the gene that transcribes mRNA.

Appendix- B

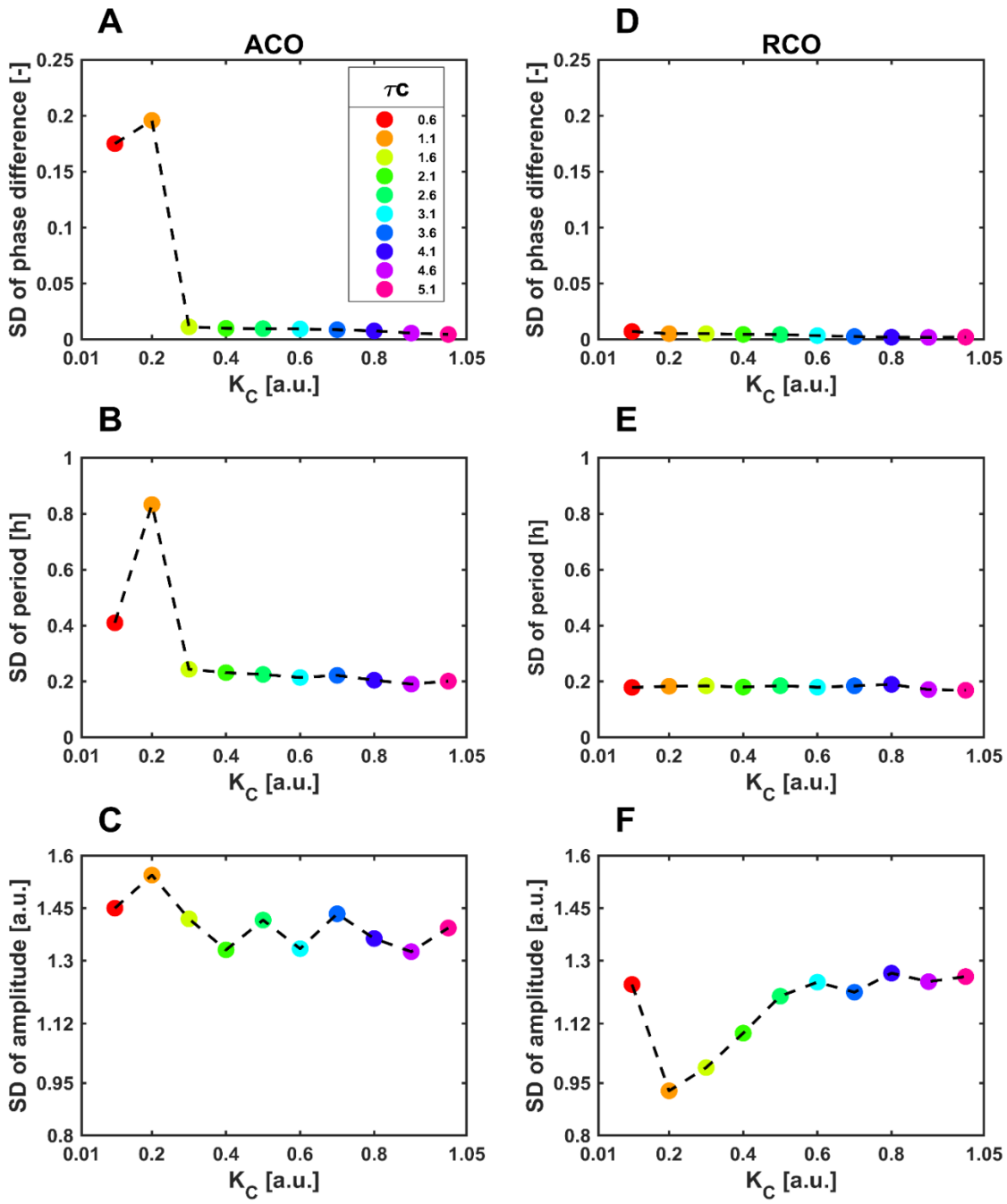

Figure S1. Robustness of the anti-phase ACO and in-phase RCO with respect to multi-parameter random perturbations. We explicitly indicated the SD values of the phase difference, period and amplitude profiles of the anti-phase ACO and in-phase RCO in Figure

4. The SDs of the phase difference, period and amplitude of the anti-phase ACO were equal to or more than those of the in-phase RCO in respective regions of *K*c.

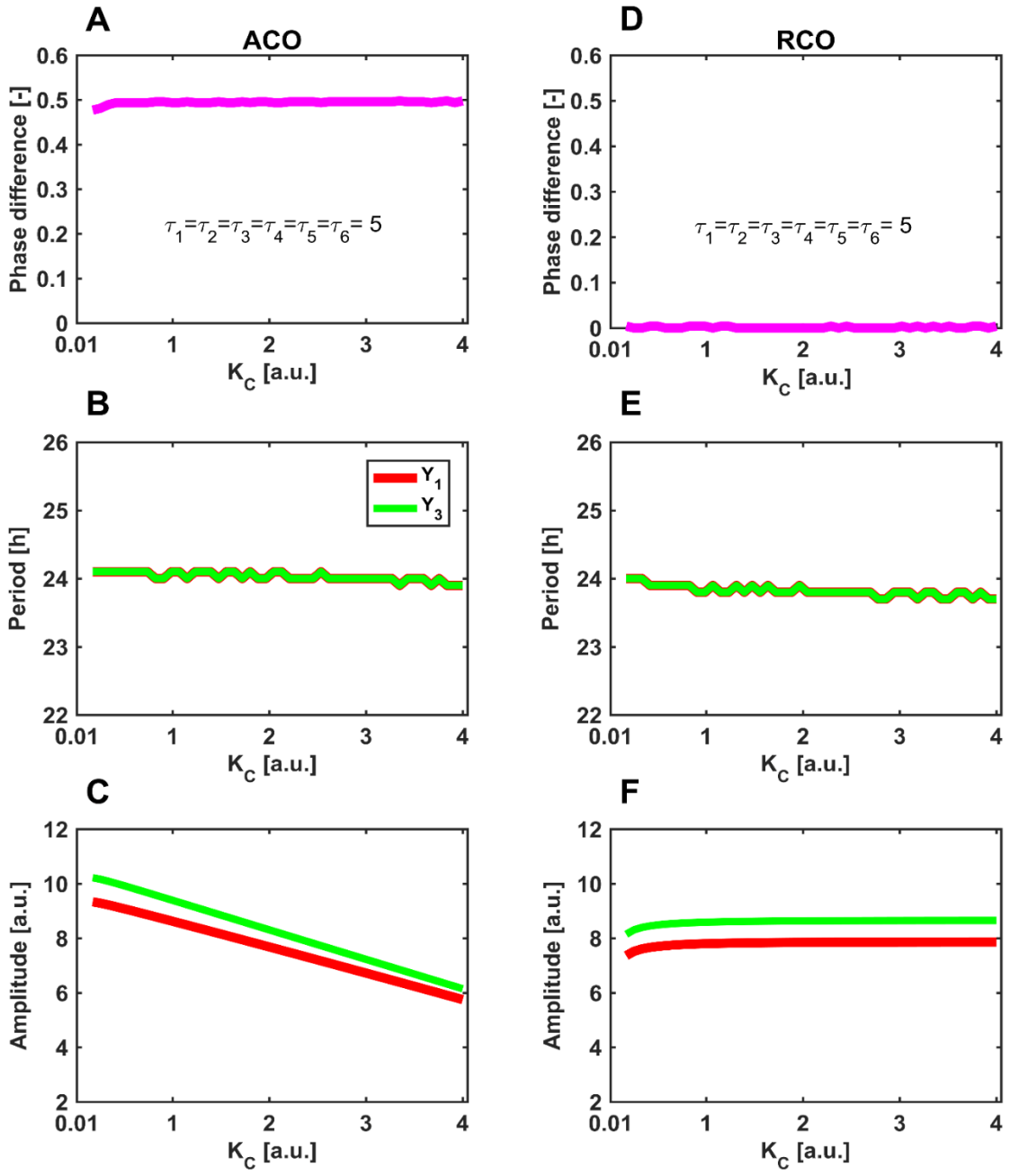

Figure S2. The phase difference, period and amplitude of the ACO and RCO models employed by the stochastic analysis. We varied the coupling dissociation constant K_C, while fixing the remaining parameter values (Table 1) and simulated the phase difference, period,

and amplitude. We used the asymACO and asymRCO. For a unique time-delay of 5 h, the ACO provided the anti-phase oscillators (A); the RCO the in-phase oscillations (D).

The periods of the anti-phase ACO and in-phase RCO showed the robustness to a change in K_C (B, E). The amplitude of the anti-phase ACO decreased with an increase in K_C (C), while the in-phase RCO determined constant amplitude (F). The amplitude of the ACO is less robust than that of the RCO.

Appendix- C

Table 6.1: Examples of experimentally verified ACO type network of biological oscillators.

Coupling Type	Organism	Network Structure	Phase	References
ACO	Zebrafish segmentation clock	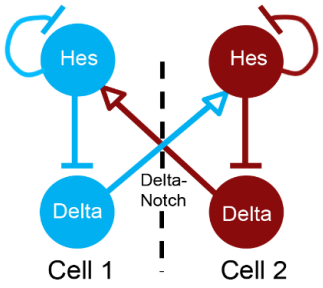	antiphase/ out-phase oscillators	(Lewis 2003, Soza-Ried, Öztürk et al. 2014, Uriu and Morelli 2017)
	Mouse mesoderm segmentation clock	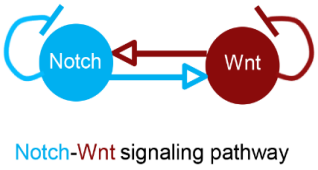	antiphase oscillators	(Kay, Harrington et al. 2017, Sonnen, Lauschke et al. 2018)
	Drosophila circadian clock	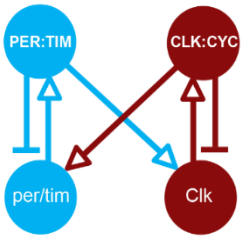	antiphase oscillators	(Glossop, Lyons et al. 1999, Cyran, Buchsbaum et al. 2003, Glossop, Houl et al. 2003)
	Mammalian circadian clock	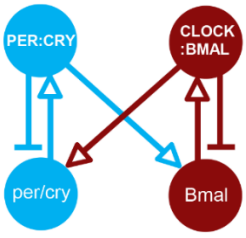	antiphase oscillators	(Relógio, Westermark et al. 2011, Battogtokh and Tyson 2018)

	SCN oscillators	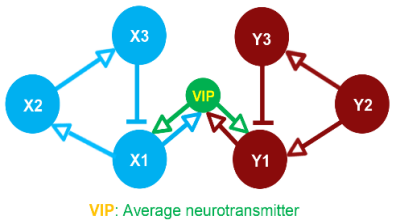	out-phase oscillators	(Gonze, Bernard et al. 2005)

Appendix- D

Entrainment ODEs of the ACO model

$$\frac{dY_1}{dt} = b_1 + k_1 \frac{K_1^{\,n}}{K_1^{\,n} + Y_2(t-\tau_2)^n} \frac{Y_4(t-\tau_5)}{K_3 + Y_4(t-\tau_5)} - (kd_1 * zeitgeber) * Y_1 \tag{5.1}$$

$$\frac{dY_2}{dt} = Y_1(t-\tau_1) - Y_2 \tag{5.2}$$

$$\frac{dY_3}{dt} = b_2 + k_2 \frac{K_2^{\,n}}{K_2^{\,n} + Y_4(t-\tau_4)^n} \frac{Y_2(t-\tau_6)}{K_4 + Y_2(t-\tau_6)} - kd_2 Y_3 \tag{5.3}$$

$$\frac{dY_4}{dt} = Y_3(t-\tau_3) - Y_4 \tag{5.4}$$

where the employed kinetic parameters are described in **Table 3.1.**

Entrainment ODEs of the RCO model

$$\frac{dY_1}{dt} = b_1 + k_1 \frac{K_1^{\,n}}{K_1^{\,n} + Y_2(t-\tau_2)^n} \frac{K_3}{K_3 + Y_4(t-\tau_5)} - (kd_1 * zeitgeber) * Y_1 \tag{5.5}$$

$$\frac{dY_2}{dt} = Y_1(t-\tau_1) - Y_2 \tag{5.6}$$

$$\frac{dY_3}{dt} = b_2 + k_2 \frac{K_2^{\,n}}{K_2^{\,n} + Y_4(t-\tau_4)^n} \frac{K_4}{K_4 + Y_2(t-\tau_6)} - kd_2 Y_3 \tag{5.7}$$

$$\frac{dY_4}{dt} = Y_3(t-\tau_3) - Y_4 \tag{5.8}$$

where the employed kinetic parameters are described in **Table 3.1.**